REVIEW

Check for updates

Carbon fibre based electrodes for structural batteries

Rob Gray,*[a] Thomas Barthelay,*[ab] Chris R. Bowen,[a] Frank Marken,[c] Alexander J. G. Lunt, [ID][a] Leif E. Asp,[d] Dan Zenkert, [ID][e] Paloma Santana Rodriguez,[a] Johanna Xu,[d] Karl Bouton[e] and Andrew T. Rhead [ID] *[a]

Carbon fibre based electrodes offer the potential to significantly improve the combined electrochemical and mechanical performance of structural batteries in future electrified transport. This review compares carbon fibre based electrodes to existing structural battery electrodes and identifies how both the electrochemical and mechanical performance can be improved. In terms of electrochemical performance achieved to date, carbon fibre based anodes outperform structural anode materials, whilst carbon fibre based cathodes offer similar performance to structural cathode materials. In addition, while the application of coating materials to carbon fibre based electrodes can lead to improved tensile strength compared to that of uncoated carbon fibres, the available mechanical property data are limited; a key future research avenue is to understand the influence of interfaces in carbon fibre based electrodes, which are critical to overall mechanical integrity. This review of carbon fibre based electrode materials, and their assembly strategies, highlights that research should focus on sustainable electrode materials and scalable assembly strategies.

[a]Department of Mechanical Engineering, University of Bath, Claverton Down, Bath, BA1 1DE, UK. E-mail: rg543@bath.ac.uk; a.t.rhead@bath.ac.uk

[b]Department of Materials, University of Oxford, Oxford, OX1 3PH, UK. E-mail: thomas.barthelay@materials.ox.ac.uk

[c]Department of Chemistry, University of Bath, Claverton Down, Bath, BA1 1DE, UK

[d]Department of Industrial and Materials Science, Chalmers University of Technology, Hörsalsvägen 7B, 41258, Göteborg, Sweden

[e]Department of Engineering Mechanics, KTH Royal Institute of Technology, SE-10044, Stockholm, Sweden

1. Introduction

Structural batteries (SBs) are a class of energy storage materials with the ability to simultaneously carry a mechanical load and store electrical energy. This bifunctionality makes them attractive as load bearing components in applications that require a combination of low mass and high energy density, such as electrified transport. By incorporating the energy storage function into the structure of the application, a separate battery

Dr Robert Gray completed his PhD in 2024 as part of the Structural Batteries group at the University of Bath (UK). His thesis was titled 'Alternative architectures for structural batteries', and his lead supervisor was Dr Andrew Rhead. Rob currently works as a Research Associate in Battery Systems at the University of Bath, where he is currently investigating thermal effects on Li-ion battery cells. He has a background in chemistry, but in recent years has become increasingly involved in the engineering aspects of battery technology.

Rob Gray

Dr Thomas Barthelay is a post-doctoral research assistant at the University of Oxford in the Department of Materials. He is currently working with Prof. Patrick Grant on novel manufacturing methods for the next generation of battery electrodes, as part of the NEXTRODE project, funded by the Faraday Institute. Thomas received his doctorate from the University of Bath, supervised by Dr Andrew Rhead, where he worked on the development of structural battery electrodes funded by GKN Aerospace. His research includes battery manufacturing, processing of solid-state electrolytes, and structural composites.

Thomas Barthelay

dedicated to energy storage is no longer needed, providing significant mass savings at a system level. The advantage of using structural batteries over traditional lithium-ion batteries (LIBs) is highlighted for the example of an electric vehicle, where a mass saving of up to 20% can be achieved if the roof panel is assembled from structural batteries instead of having the roof panel and a separate traditional LIB for energy storage.[1] When using the Web of Science to search for research publications with the term "structural batt*" in the title, 1709 publications are returned, including 199 in 2023 alone, showing a year-on-year increase of 23% on average since 2013, as visualised in Fig. 1.

SBs can be divided into two different types: (i) top-down developed SBs, which consist of off-the-shelf LIBs that have been mechanically reinforced with other components,[2] and (ii) bottom-up developed SBs, which are assembled from active battery materials that also have the appropriate mechanical properties.[3] Whilst top-down developed SBs are now being

realised commercially,[4] bottom-up SBs are at a lower technology readiness level; this is a consequence of the increased complexity in the development of active battery materials with appropriate mechanical properties. Despite this challenge, bottom-up developed SBs offer the greatest potential for mass savings and an associated increase in the driving or flying range since the active battery materials used in their assembly possess both mechanical and electrochemical properties intrinsically, thereby eliminating the need for additional structural reinforcements.

The review will examine bottom-up developed SBs, which rely on materials that are both electrochemically active and mechanically effective. As such, this review focuses on the particularly promising form of SBs based on carbon fibres.[5] Current state-of-the-art SBs consist of a carbon fibre anode and lithium iron phosphate (LFP) cathode, which are separated by a glass fibre separator and all embedded in a biphasic
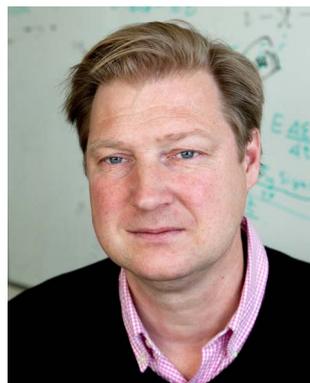
Frank obtained a Dr rer. nat. degree at RWTH Aachen (Germany) and was a Feodor-Lynen Fellow at La Trobe University, Melbourne (Australia). He worked as a Stipendiary Lecturer at Oxford and at Loughborough University (UK). In 2004 he moved to the University of Bath. In 2011 he was promoted to a personal chair in physical chemistry. His research is linked to the Institute of Sustainability (IoS) and the Water Innovation Research Centre (WIRC) at Bath and focused on pure and material electrochemistry, electroorganic processes, and energy storage.

Frank Marken

Dan Zenkert is a professor in Lightweight Structures at the Department of Engineering Mechanics at the Royal Institute of Technology (KTH) in Stockholm, Sweden. His current research focus is on structural batteries and multifunctional composites. He has been working on multifunctional carbon fibre composites since around 2010 with a special focus on structural battery composites but lately also on adding other functions, such as sensing, shape-morphing and energy harvesting through the coupling of mechanics and electrochemistry.

Dan Zenkert

Dr Leif Asp holds the chair as professor in lightweight composite materials and structures at the Division of Material and Computational Mechanics at the Department of Industrial and Materials Science at Chalmers University of Technology in Gothenburg, Sweden. Dr Asp's research group performs research on multifunctional composites, with focus on structural battery composites, a material that can simultaneously store electrical energy and carry mechanical loads. The work comprises material development, modelling, and characterization, where the coupled electro-chemo-mechanical processes in the structural battery cells are studied.

Leif E. Asp

Dr Andrew Rhead is an associate professor/senior lecturer in the Department of Mechanical Engineering and a member of the Centre for Integrated Materials, Processes & Structures at the University of Bath in the UK. His background is in design, manufacture and performance of carbon fibre composite structures. He has led the University of Bath Structural Batteries team since 2019. Structu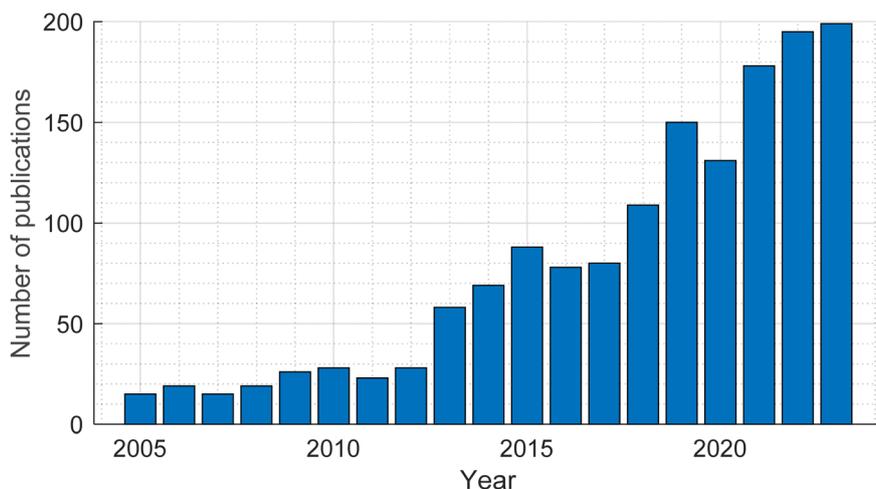ral batteries are able to carry mechanical load whilst acting as energy storage materials, and the team focuses on fibre-based electrode development, cell architectures and manufacturing scale up via experiments and modelling.

Andrew T. Rhead

Fig. 1 The number of publications each year with the term "structural batt*" in the publication title, since 2005.

electrolyte matrix to form a composite, as shown in Fig. 2a. In this case the cathode does not provide any structural properties.

The mechanical stiffness and strength of the battery are provided by the carbon fibre anode and the glass fibre separator, which have a comparatively high Young's modulus of 290 GPa and 76 GPa and tensile strength of 3.1 GPa and 1.7 GPa, respectively.[8] The mechanical load is transferred between the fibres within the composite by the SB electrolyte, which acts as a matrix.

For a structural battery to be considered for an application, such as a two-seater electric aircraft designed for 60 minutes of flight, a minimum energy density of 52 W h kg^{-1} and a minimum power density of 103 W kg^{-1} would be required.[9] Current state-of-the-art SBs have a lower energy density of 41 W h kg^{-1} and a power density of 12 W kg^{-1}, demonstrating that current SBs fail to meet these requirements, in particular in terms of power density.[6] To improve the energy and power density, a hypothetical next-generation SB based on carbon fibre based electrodes (CFBEs) is shown in Fig. 1b; in this case carbon fibres are used to reinforce both the cathode and anode. CFBEs are a class of electrode materials with the potential to provide a greater energy and power density than current state-of-the-art SB electrode materials. CFBEs are composites that comprise high strength and stiffness carbon fibres that are individually coated in high-

capacity electrode materials, with the carbon fibre acting as both a current collector and providing structural support for the coating. For the anode, carbon fibre based anodes (CFBAs) have much greater capacities than existing carbon fibre structural anodes due to the high capacity of the coating material. For the cathode, carbon fibre based cathodes (CFBCs) offer a pathway to create the first truly structural cathodes due to the presence of the carbon fibre reinforcement.

The aim of this review is to highlight the potential of CFBEs as next generation SB materials and to indicate avenues for further research. Topics considered include the range of active materials that have been coated onto carbon fibres in CFBAs and CFBCs, the strategies employed to achieve high capacity and long cycle life electrodes, the potential scalability and sustainability outlook for these materials, and pathways for integration into complete cells.

2. Methodology for the assembly of carbon fibre based electrodes

2.1. Overview

The method and conditions used to coat the electrode material onto carbon fibres to produce CFBEs have a significant impact
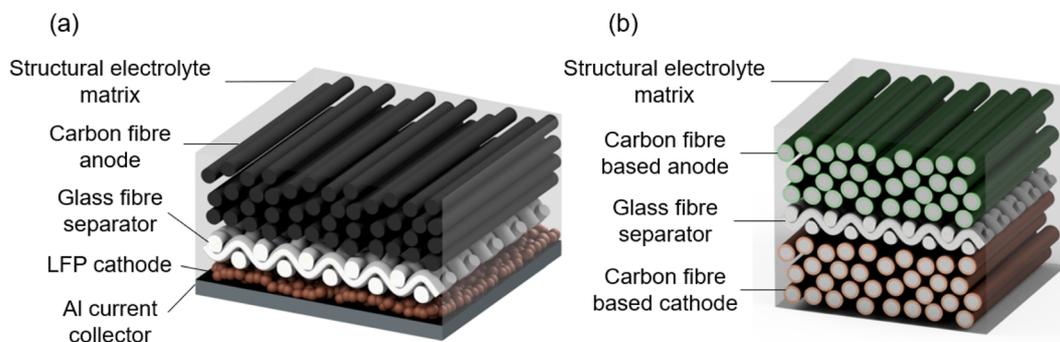

Fig. 2 (a) Illustration of the current state-of-the-art structural battery (SB)[6,7] and (b) potential future SB with a laminated architecture using carbon fibre based electrodes (CFBEs) for improved mechanical and electrochemical performance. As an indicator of scale, the diameter of an individual carbon fibre is typically 10 μm.

on the electrochemical and mechanical performance of the electrode. Most assembly strategies for CFBEs adopt a two-step process involving a pre-treatment step, which modifies the surface of the carbon fibre to make it suitable for coating, followed by a coating step where the electrode material is applied to the fibre surface. In this section, the effectiveness of CFBE assembly strategies and how CFBEs can be combined with other battery components to produce a structural battery composite are outlined.

2.2. Pre-treatment of carbon fibres

Good adhesion between the carbon fibre reinforcement and the coated electrode material is critical to both the mechanical properties of the composite for load transfer purposes, good electrochemical performance, and for high electronic conductivity between the fibre and coating. One method to improve the degree of adhesion between the carbon fibre and the electrode coating is through a process of functionalisation; this is a pre-treatment stage that introduces oxygen containing functional groups, such as carbonyls and carboxylic acids, to the surface of the carbon fibre, which increases the degree of covalent bonding between the carbon fibre and coating.[10] While several different methods for functionalisation exist, which include chemical oxidation,[11] gas-phase oxidation[12] and plasma treatment,[13] the process of chemical oxidation using acids has been used almost exclusively for the pre-treatment of carbon fibres for use in CFBEs. The range of conditions used to functionalise carbon fibres that have been successfully used in CFBEs to date are summarised in Table 1.

The most frequently used acid for functionalisation by chemical oxidation is a combination of nitric acid (HNO_3) and sulphuric acid (H_2SO_4). However, this combination of acids has been shown to lead to a 12.5% loss in the tensile strength of the carbon fibre.[14] The addition of phosphoric acid (H_3PO_4) to the HNO_3 and H_2SO_4 acid mixture has been shown to reduce the negative effect of chemical oxidation on the carbon fibre tensile strength to reduce the loss in strength to only 3%. This is likely to be due to the H_3PO_4 preventing the overoxidation of carbon fibres by protecting C–C bonds from being cleaved.[11]

Another carbon fibre surface feature that can affect the interface of a coated electrode material is its sizing; this is a thin polymer coating that is applied to carbon fibres after manufacture to make them easier to handle while promoting thorough fiber impregnation and bonding between the fibre and the resin. Currently, it is unclear to what extent sizing affects electrochemical and mechanical performance in CFBEs; however, the majority of publications on SBs use unsized or desized fibres, which can be produced from sized fibres by removing the sizing using solvents in a Soxhlet extractor[28,29] or an agitated bath.[30,31]

2.3. Coating of carbon fibres

After pre-treatment of the carbon fibres, an electrode coating needs to be applied. To date, four methods have been used to coat electrode materials onto carbon fibres for use in CFBEs. The process of precipitation involves the growth of a precursor material on the carbon fibre in a solution bath which is followed by annealing, which involves a high temperature treatment to produce the desired electrode material coating.[16] Hydrothermal synthesis is similar to precipitation except that higher temperatures and pressures are required to grow crystals on the carbon fibre surface.[24] Electrophoretic deposition (EPD) requires the application of an electric field across a solution that attracts charged particles and it coats them onto the carbon fibres which are oppositely charged.[32] The process of slurry coating involves drawing a doctor blade over an electrode slurry to evenly coat one surface of a carbon fibre tow with electrode material.[33] A comparison of these methods is described below and summarised in Table 2.

In terms of energy requirements, both precipitation and hydrothermal synthesis are energy intensive processes due to high annealing temperatures, where temperatures of 400 °C for 2–3 hours are typical.[15,17,25] Hydrothermal synthesis has additional energy costs associated with the temperatures required to initially grow crystals on the carbon fibre surface. The processes of EPD and slurry coating, while being less energy intensive coating processes compared to precipitation and hydrothermal synthesis, have a large amount of embedded energy in the electrode material particles that are being coated, since they are often made via hydrothermal processes,[34] which partly cancels out their benefit in terms of energy requirements. These high energy requirements also make these processes less sustainable.

For scalability considerations, hydrothermal synthesis and precipitation can require inert atmospheres of nitrogen gas (N_2)[15] or argon (Ar)[25] for the annealing stage, and hydrothermal synthesis requires an autoclave to achieve elevated pressures, making it more difficult to achieve a continuous process with

Table 1 Conditions for the chemical oxidation of carbon fibres for the assembly of CFBEs. Tensile strength data are from Feng *et al.* and were measured by integrating single-fibre tensile data through a two-parameter Weibull model.[14]

Acid used	Acid ratio	Temp. (°C)	Time (h)	Tensile strength loss (%)	Ref.
$H_3PO_4 : HNO_3 : H_2SO_4$	(1 : 3 : 9)	60	1	3.03	14–17
$HNO_3 : H_2SO_4$	(1 : 3)	60	1	12.46	14, 18 and 19
$HNO_3 : H_2SO_4$	(3 : 1)	80	24	—	20–23
$HNO_3 : H_2SO_4$	(1 : 3)	80	3	—	24
$HNO_3 : H_2SO_4$	(3 : 1)	25	12	—	25
$HNO_3 : H_2SO_4$	(3 : 1)	80	12	—	26
HNO_3	(1)	65	2	—	27

Table 2 A comparison of the different coating methods used to produce CFBEs

Coating method	Energy requirements/sustainability	Scalability	Performance	Cost
Precipitation	High	Medium	High	Medium
Hydrothermal synthesis	High	Low	High	High
Electrophoretic deposition (EPD)	Low[a]	High	High	Medium
Slurry coating	Low[a]	Very high	Medium	Low

[a] The energy requirements for EPD and slurry coating are low but the materials used have a greater embedded energy.

these methods. However, it has been demonstrated that it is possible to hydrothermally produce a SnO_2-based CFBA without an annealing stage, highlighting that scalability is more feasible for some material combinations.[20] EPD does not require special conditions and is faster than hydrothermal synthesis and precipitation, making it a favourable choice in terms of scalability.

Slurry coating is the most scalable method since the method is currently used by the battery industry to coat electrode materials onto current collectors.[35] However, the process only coats one surface of the carbon fibre tow, unlike the other methods which individually coat carbon fibres. This places slurry coating at a disadvantage in terms of both electrochemical and mechanical performance as the interfacial surface area between the fibres and the coating is smaller. Dip coating is a form of slurry coating that does achieve coating of individual fibres, and has been used to produce LFP-based CFBCs,[36] but this is less scalable than conventional slurry coating due to the additional handling steps. In terms of cost, hydrothermal synthesis is the most expensive, requiring an autoclave and an inert atmosphere, while precipitation and EPD are less expensive, requiring an inert atmosphere and potentiostatic electrochemical setup, respectively. The next sections describe carbon fibre based anodes and cathodes.

3. Performance of carbon fibre based anodes

3.1. Introduction to carbon fibre anodes

Due to a combination of high reversible capacity and high Young's modulus, intermediate modulus polyacrylonitrile (PAN)-based carbon fibres are the most widely used class of anode materials in SBs.[37] A carbon fibre is an example of an intercalation-type anode material, where energy storage is achieved by reversibly accommodating Li^+ ions in vacant sites within their atomic structure. Carbon fibre anodes contain graphitic regions, where Li^+ ions can intercalate and deintercalate between layers of graphene during charging and discharging cycles, as shown in Fig. 3a. In carbon fibres, Li^+ ions can also be inserted into non-graphitic regions, similar to how Li^+ ions are inserted into disordered carbons.[38]

The reversible capacity of a carbon fibre anode is up to 37% lower than that of graphite,[37] which is the most widely used anode material in conventional LIBs. The capacity of carbon fibre anodes can be increased by coating the carbon fibre with conversion-type anode materials; these are materials which are characterised by their ability to reversibly react with Li^+ ions to form a crystal matrix that contains solid metal nanoparticles. The change in structure of conversion-type anodes during
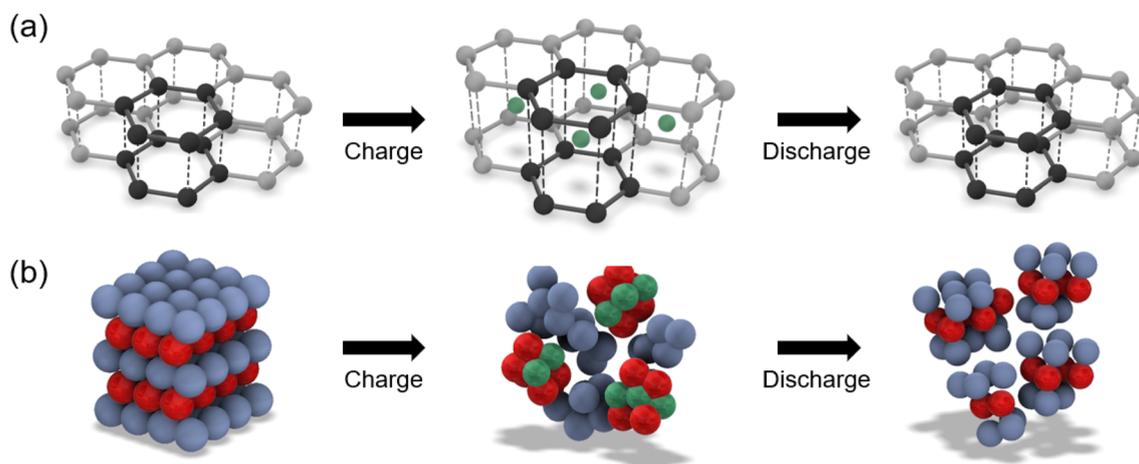

Fig. 3 Illustration of the effect of charging and discharging on (a) graphite, an intercalation-type anode and (b) SnO_2, a conversion-type anode. Green spheres are Li^+ ions, black/grey spheres are carbon, red spheres are O^{2-} ions, and blue spheres are Sn^{4+} ions/Sn metal. In the case of the conversion-type anode, the illustration shows the material going from a pristine state prior to charging to a pulverised state after the first discharge.

charging and discharging is illustrated in Fig. 3b. The theoretical capacity, which is the calculated maximum specific energy density of an electrode material, is much higher for conversion-type anode materials than for intercalation-type anode materials, allowing higher reversible capacities to be achieved.

As carbon fibres are both an anode material and a structural material, any coating used to create a CFBA must be justified by improvements in electrochemical and/or mechanical properties. This section explores the impact of using different coating materials on the electrochemical and mechanical properties of CFBAs.

3.2. Electrochemical properties

3.2.1. Comparison of carbon fibre based anodes. Table 3 summarises the electrochemical performance of CFBAs that have been reported in the literature to date. Due to overlap in the potentials of Li^+ ion intercalation in carbon fibres and the conversion reaction in a coated material, both the coating and the carbon fibre participate in energy storage on the anode side, thereby increasing the reversible capacity.[25] Conversion-type anode materials used as coatings in CFBAs possess much greater theoretical capacities than the carbon fibre,[37,48] which indicate that CFBAs have greater theoretical capacities than carbon fibre anodes.

3.2.2. Reversible capacity of carbon fibre based anodes (CFBAs). The first cycle coulombic efficiency (CE) of the CFBAs ranges from 54% to 70%, which is comparable to the value of 63% found for a pristine carbon fibre. Fig. 4 presents plots that compare the reversible capacity of CFBAs to other important parameters such as the electrode theoretical capacity, coating mass fraction, which is the percentage of CFBA mass that is the

coating, and coating volume fraction, which is the percentage of the total CFBA volume that is the coating. Unlike carbon fibre anodes, which typically deliver reversible capacities that are less than half of their theoretical capacity, reversible capacities of CFBAs often exceed their theoretical capacity, as shown in Fig. 4a where reversible capacities of CFBAs above the dotted line exceed their theoretical capacity. Fig. 4a also shows that CFBAs with greater theoretical capacities generally have greater reversible capacities, indicating the expected importance of theoretical capacity in the electrochemical performance.

For some of the CFBAs, such as those using SnO_2 as a coating, theoretical capacity is exceeded as a result of the coated conversion-type anode material reversibly reacting further with Li^+ ions *via* an alloying reaction.[49] The presence of this alloying reaction can be seen in the cyclic voltammetry (CV) plots in Fig. 5. Fig. 5a, which shows the first three cathodic and anodic sweeps for a carbon fibre anode, shows a peak at 0.35 V (*vs.* Li/Li^+) in the first cathodic sweep that corresponds to solid electrolyte interphase (SEI) formation at the anode surface. The SEI is a passivating layer that forms on the surface of the anode during the first charge cycle, and is formed from the reduction of electrolyte components, due to the instability of the electrolyte in the full voltage operating window of the cell. The broad cathodic sweep that increases approaching 0 V (*vs.* Li/Li^+) in all three cycles is the intercalation of Li^+ ions into the carbon fibre anode. The broad peaks between 0 and 1 V (*vs.* Li/Li^+) in the anodic sweeps are ascribed to the deintercalation of Li^+ ions from the carbon fibre anode, showing the reversibility of this process.

Fig. 5b shows the first three cathodic and anodic sweeps for a CFBA consisting of SnO_2 coated carbon fibres. The cathodic

Table 3 Comparison of the electrochemical properties of different CFBAs. Values left blank are unknown information about the coatings that could not be obtained from the data, except in the case of an uncoated carbon fibre, which has been included for comparison

| Coated anode material	Theoretical capacity (mA h g^{-1})	Type of carbon fibre	Conductive additive	Coating thickness (nm)	Coating mass fraction (wt%)	Coating volume fraction (%)	Initial CE (%)	Reversible (theoretical) capacity (mA h g^{-1})	Cycle rate (mA g^{-1})	Cycles	Ref.
None	—	PAN-based	—	—	—	—	63%	177 (372)	100	10	30
SnO$_2$	782 (ref. 39)	PAN-based	rGO	35	—	3	61%	313	20	100	15
		PAN-based	rGO	70	—	5	61%	369	100	100	16
		Bamboo	Glucose	140	43.66	8	—	627 (551)	100	100	25
		PAN-based	None	50–70	10.43	3	59%	510 (414)	100	150	20
		PAN-based	MOF	80–100	18.46	—	54%	732 (448)	100	150	18
Co$_3$O$_4$	890 (ref. 40)	PAN-based	MOF	200	6.22	11	63%	420 (404)	100	150	41
		PAN-based	None	100	23.6	5	69%	625 (494)	100	150	21
ZnO	978 (ref. 42)	Unknown	MOF	100	32.9	5	58%	510 (571)	100	300	26
		Unknown	MOF	100	32.9	5	—	395 (571)	2000	1000	
ZnCo$_2$O$_4$	868 (ref. 43)	PAN-based	None	140–160	45.42	9	66%	787 (597)	100	150	19
		PAN-based	None	140–160	45.42	9	—	290 (597)	2000	10	
		PAN-based	MOF	—	15.1	—	66%	463 (447)	50	100	17
Fe$_3$O$_4$	925 (ref. 44)	PAN-based	None	—	—	—	69%	740	100	100	27
		PAN-based	None	—	—	—	—	503	500	500	
MnO	756 (ref. 44)	Cotton	Polypyrrole	—	72.7	—	70%	829 (650)	200	200	45
		Cotton	Polypyrrole	—	72.7	—	—	429 (650)	3000	10	
MnO$_2$	1230 (ref. 46)	Unknown	None	90	43.47	4	60%	648 (745)	100	150	23
Mn$_3$O$_4$	937 (ref. 44)	PAN-based	None	70	37.90	—	60%	611 (586)	100	150	24
NiO	718 (ref. 47)	PAN-based	None	—	—	—	67%	648	100	150	22
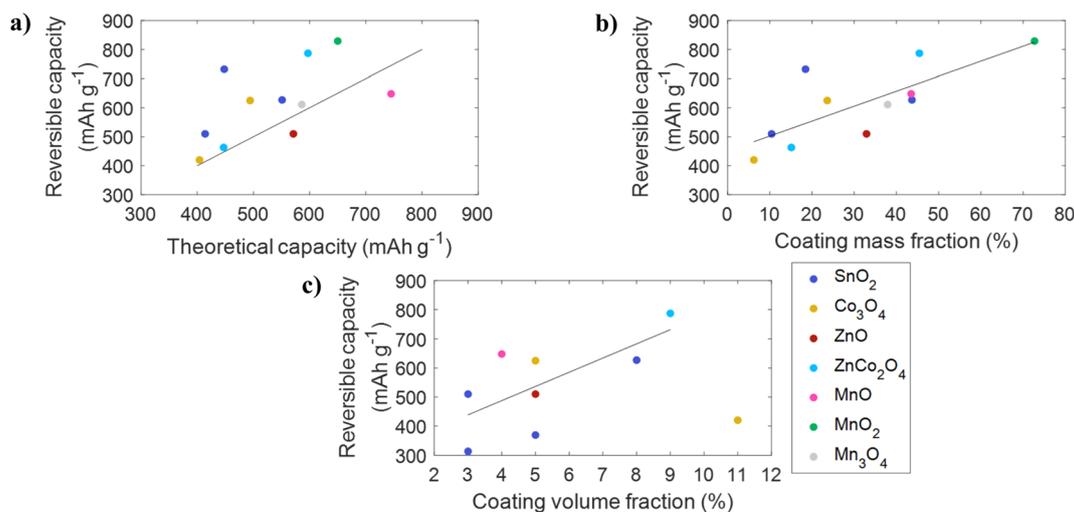
Fig. 4 Plots showing how reversible capacity of CFBAs changes with (a) electrode theoretical capacity, (b) coating mass fraction and (c) coating volume fraction. Each data point is for a different study of a CFBA material. Note that in (a) the line is $x = y$, and in (c) the electrode with a coating volume fraction of 11% is not included in the trendline.
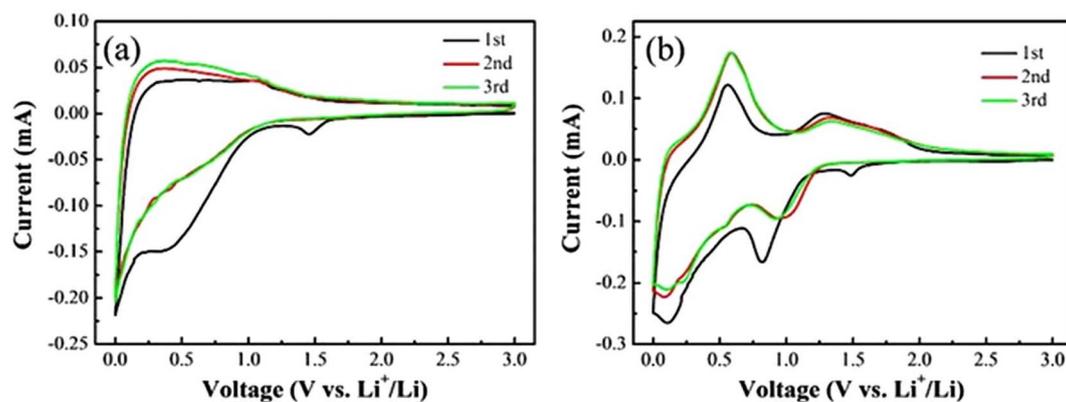

Fig. 5 Cyclic voltammetry plots for the first three cycles of (a) carbon fibre anodes and (b) a CFBA consisting of SnO$_2$ coated carbon fibres.[25] Reproduced from ref. 25 with permission from Elsevier, copyright 2024.

peak at 0.65 V (*vs.* Li/Li$^+$) in the first cycle, and peaks at 0.95 V (*vs.* Li/Li$^+$) in subsequent cycles, correspond to conversion of SnO$_2$ to Sn and LiO$_2$. The cathodic peak at 0.1 V (*vs.* Li/Li$^+$) in all cycles is ascribed to the alloying of Sn to Li$_x$Sn. These processes are then reversed during the anodic sweep, with the peaks at 0.55 V and 1.3 V (*vs.* Li/Li$^+$) corresponding to dealloying and deconversion, respectively. This is how the capacity of a CFBA with a SnO$_2$ coating can exceed its theoretical capacity, as the alloying reaction, that is shown to be occurring from the CV plots, is not factored into the theoretical capacity determination.

The factors affecting the theoretical capacity of CFBAs are the mass fraction of the coating and the theoretical capacity of the coated anode material. Fig. 4b shows that the reversible capacity of a CFBA increases linearly with increasing mass fraction of the coated anode material. This is promising since the increase in reversible capacity would have been expected to fall with increasing mass fraction as the use of thicker

electrodes can introduce mass transport limitations that reduce capacity improvements.[50] Similarly, an increase in reversible capacity with coating volume fraction is observed, with no indication of a decrease in reversible capacity at higher coating volume fractions, as shown in Fig. 4c.

These results indicate that current CFBAs are sufficiently thin (low volume fraction) or of low-density (low mass fraction) to avoid mass transport limitations during cycling. This suggests that, at least on the nanometre scale, coating mass fractions and volume fractions can be increased further without compromising reversible capacity. A comparison of reversible capacity with the coating mass fraction or volume fraction for a specific material and coating method would be of interest to fully characterise the relationship between these variables for CFBAs.

Conversion-type anode materials, despite having high theoretical capacities, have seen limited commercial use. This is a result of large volume changes that occur during cycling,

which leads to pulverisation of anode particles and a gradual decrease in the capacity, resulting in a loss of capacity over many cycles.[51] However, in the CFBAs observed in Fig. 4, the reversible capacities are excellent due to a synergistic effect between the carbon fibre and the coated conversion-type anode material, which arises as a result of the carbon fibre acting as a high surface area substrate that alleviates the effects of reversible volume expansion in conversion-type materials.[21]

3.2.3. Power density of CFBAs.
The ability of CFBAs to deliver a high reversible capacity at high cycling rates is critically important since the specific power density of structural batteries is the electrochemical property that requires the greatest improvement.[6] Several of the CFBAs in Table 3 have been tested at high power densities, notably those with cycle rates of 2000 mA g^{-1} or greater. In this regard, the C-rate is a measurement of the cycling rate relative to the theoretical capacity of an electrode material and has units of h^{-1}; for example, a C-rate of 1C indicates that the battery is charged from 0–100% in one hour. A C-rate of greater than 4C is classified as fast charging by commercial LIB standards,[52] and therefore an anode material that demonstrates a high reversible capacity at C-rates in this range would be desirable. An MnO-based CFBA was able to deliver a reversible capacity of 429 mA h g^{-1} at 4.6C, which represents a cycling rate of less than 15 minutes.[45] By comparison, a carbon fibre anode was able to deliver only 177 mA h g^{-1} at 0.25C, which is over 30 times slower.[30]

Other examples of exceptional power density in CFBAs are observed for those based on ZnO and ZnCo$_2$O$_4$, which achieved reversible capacities of 395 mA h g^{-1} and 290 mA h g^{-1}, respectively, at C-rates of greater than 3C.[19,26] Notably, the ZnO-based CFBA was able to deliver this battery performance after 1000 cycles. Interestingly, the coating mass fraction does not seem to detrimentally impact the ability of a CFBA to deliver high reversible capacities at high C-rates, as the MnO-based CFBA possesses the highest coating mass fraction whilst being operated at the highest C-rate of all CFBAs. It would be beneficial to compare the effects of important properties, such as the coating volume fraction and porosity, on the ability of CFBAs to deliver high reversible capacities at high C-rates, to allow the power density of CFBAs to be optimised.

3.2.4. Coating morphology of CFBAs.
The morphology of CFBA coatings is a property that is important for the electrochemical performance of the anode, and is difficult to characterise quantitatively. CFBAs have been produced with a wide range of morphologies, some of which are shown in Fig. 6. A uniform coating of the active material is crucial for optimizing electrochemical performance, promoting even transport, preventing mechanical degradation, and ensuring consistent electrical conductivity. This uniformity enhances the battery's
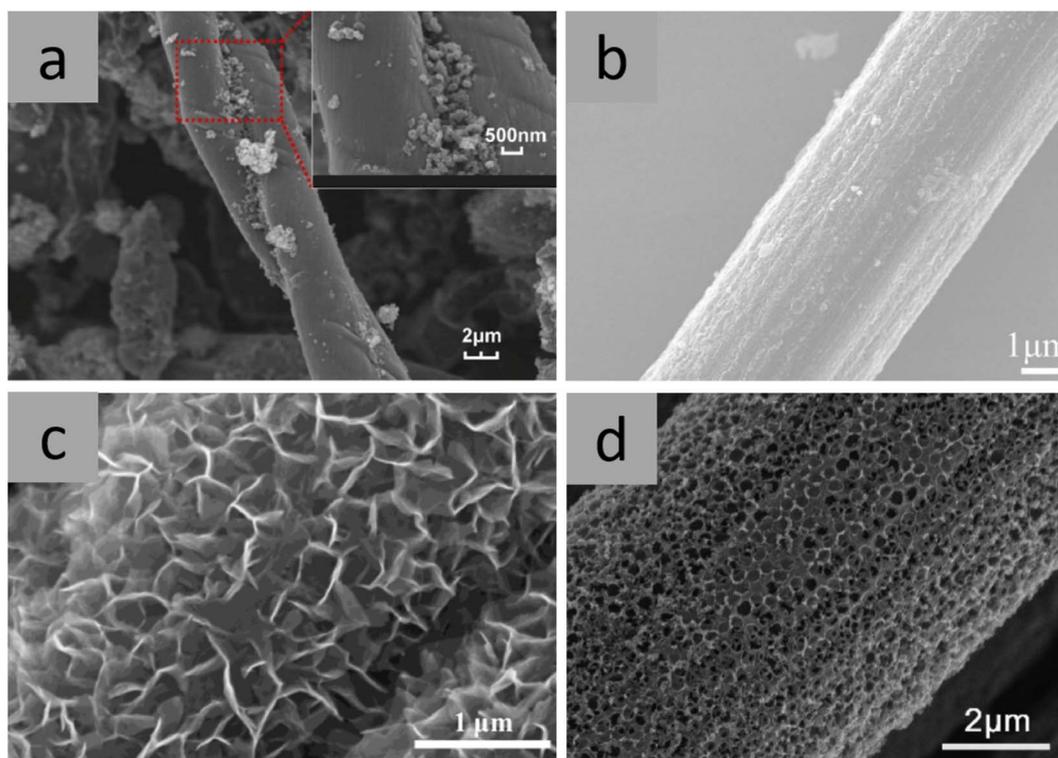

Fig. 6 Scanning electron microscopy (SEM) images of CFBAs with different coating morphologies, including (a) inhomogeneous MnO,[45] (b) homogeneous Co$_3$O$_4$,[21] (c) V$_2$O$_5$ nanosheets,[53] and (d) macroporous MoS$_2$.[54] The void spaces in the MoS$_2$ coating were created by including polystyrene spheres in the coating that thermally decompose during annealing, demonstrating a creative use of the annealing process during the coating step. (a) Reproduced from ref. 45 with permission from Elsevier, copyright 2024. (b) Reproduced from ref. 21 with permission from Springer Nature, copyright 2024. (c) Reproduced from ref. 53 with permission from Elsevier, copyright 2024. (d) Reproduced from ref. 54 with permission from Wiley, copyright 2024.

efficiency and cycle life. However, this trend is not seen in the data since the MnO-based CFBA with a highly inhomogeneous coverage of the carbon fibre surface, shown in Fig. 6a, exhibits the highest reversible capacity out of all CFBAs.[45] The homogeneity of the coating is likely to be more important for mechanical performance, which is discussed in the next section.

Another important property of the coating morphology is the porosity level. The Co_3O_4 coating in Fig. 6b contains mesopores 2.18 nm in diameter, which increases the surface area of the coating. A larger surface area provides improved contact between the electrolyte and the electrode, thereby increasing the amount of active material, and consequently improving the reversible capacity of the CFBA.[21] The presence of larger pores in synthesised macroporous coatings, such as the V_2O_5 nanosheet coating and MoS_2 coating shown in Fig. 6c and d, respectively, result in a smaller surface area. However, a secondary advantage of providing void spaces is that they can help accommodate expansion of anode particles during conversion reactions, as in Fig. 6b, thereby contributing to reducing the effect of pulverisation and thus maintaining the long-term reversible capacity of the CFBA.[54]

3.2.5. Coating additives for CFBAs. In CFBAs, an electrically conductive additive is added to improve the electronic conductivity, since the electronic conductivity of most conversion-type anode materials is low.[55] Another reason for the low electronic conductivity in battery electrodes is the binder material, that is essential for structural integrity, but is also insulating. However, CFBAs do not contain binders due to the synthesis methods used. The most common method for introducing a conductive additive is through the use of metal organic frameworks (MOFs); these are crystal structures that comprise metal ions and coordinated organic ligands which can be synthesised as an intermediate on the surface of the carbon fibre using a precipitation coating method.[17,18,26,41] During the annealing step, metal ions in the MOF form the anode coating, and the organic component of the MOF subsequently carbonises to form a porous carbon matrix. The increase in porosity and the introduction of conductive carbon both contribute to increasing the amount of active material in the coating.[56]

As an alternative to MOFs, organic compounds such as glucose[25] and polypyrrole[45] have been similarly used as compounds that carbonise to form an electrically conducting network during an annealing step. Equally, the electronic conductivity can be improved by inclusion of reduced graphene oxide (rGO) sheets within the coating. The rGO sheets act as electrically conducting pathways and create void spaces between the sheets, which mitigate the effect of volume changes in the anode particles.[15,16] The addition of rGO to a coating containing SnO_2 prevented rapid loss in reversible capacity after 60 cycles as a result of the rGO countering the effects of pulverisation.[15] Carbon nanotubes, attached perpendicular to the surface of carbon fibres, have also been proposed exclusively for creating void space.[57] It is worth noting that many CFBAs have been able to deliver excellent electrochemical performance without the use of additive compounds, and ultimately, additive compounds should only be employed when the performance of the CFBA has been deemed unsatisfactory without them as they may contribute unnecessary 'dead weight' to the composite.

3.3. Mechanical properties of CFBAs

3.3.1. Effect of the coating material. While the electrochemical properties of CFBAs have been explored in a relatively high number of publications, there are significantly fewer studies investigating mechanical properties of CFBAs; see Tables 3 and 4. Tensile strength and elastic modulus are the only mechanical properties of CFBAs that have been determined by tensile testing to date. Following initial work by Jacques et al.,[58] Duan et al.[59] characterised the effects of lithiation on the elastic moduli and volume change of single IMS65 carbon fibres. Duan[59] and co-workers found the modulus in the radial direction to double upon lithiation, whereas they found a small reduction of 13% in the modulus in the axial (longitudinal) direction. For coatings with no additive compounds, CFBAs were found to have both a lower tensile strength and lower elastic modulus compared to pristine carbon fibres.[15,16,24] Some of this loss in mechanical properties can be attributed to the acid functionalisation process during a pre-treatment step. However, the resulting tensile strength reduction is a maximum of 12.5%,[14] which is less than the loss observed for additive-free SnO_2-based CFBAs. Hydrothermal synthesis and annealing processes during the coating step may have further reduced the tensile strength of the carbon fibre through the introduction of surface defects.[15] Nevertheless, it can be concluded that the coating material is likely to have an effect on mechanical

Table 4 Comparison of the mechanical properties for different CFBAs. Percentages in brackets are the change from that of a pristine carbon fibre in each respective study. All data are for pristine samples prior to cycling

Coating of interest	Testing method	Coating	Tensile strength (GPa)	Elastic modulus (GPa)	Shape parameter	Scale parameter (GPa)	Ref.
SnO_2/MOF	Tensile	SnO_2/MOF	3.91 (−22%)	212 (−12%)	—	—	19
Mn_3O_4	Tenslie	Mn_3O_4	4.67 (−8%)	195 (−6%)	—	—	24
SnO_2/rGO	Single-fibre Weibull model	SnO_2	2.87 (−33%)	—	4.36 (−45%)	3.14 (−31%)	15
		rGO	4.54 (+6%)	—	4.52 (−43%)	4.97 (+10%)	
		SnO_2/rGO	4.37 (+2%)	—	7.87 (−1%)	4.63 (+2%)	
SnO_2/rGO	Single-fibre Weibull model	SnO_2	3.18 (−23%)	—	5.24 (−1%)	3.40 (−24%)	16
		SnO_2/rGO	4.73 (+14%)	—	7.84 (+48%)	5.01 (+11%)	

properties of the CFBA due to the wide range of tensile strengths found for different coatings. Therefore, a study to determine the mechanical properties of the CFBA during each stage of the assembly would be useful for decoupling the effects of different processing steps.

An SnO_2 CFBA using a MOF as a conductive additive exhibited lower mechanical properties than the uncoated carbon fibre. However, the use of rGO as an additive improved the tensile strength of the carbon fibre by 6%. This benefit is thought to be a consequence of the wrinkled and interleaved nature of the rGO sheets, which are less rigid than other coatings. The sheets were able to straighten out and slide over one another as the composite is loaded under tension, thereby reducing the stress imposed by rGO on the surface of the carbon fibre during this process.[16]

One disadvantage of rGO coated carbon fibres is their relatively wide distribution of tensile strengths compared to uncoated carbon fibres. This is indicated by the small Weibull shape parameter and a result of inhomogeneous rGO coating. SnO_2 and rGO coated carbon fibres have a distribution of tensile strengths that are more typical of uncoated carbon fibres, indicating that the addition of SnO_2 improves the dispersion of rGO on the surface.[15] Fig. 7 shows the effect that adding rGO to SnO_2 has on the Weibull plot and stress–strain curve, when compared to pristine carbon fibres or those coated only in rGO. This highlights the synergistic effect of combining rGO with conversion-type anode materials to improve both the mechanical properties and electrochemical performance. An important mechanical property that is missing from studies is the fibre-to-coating adhesion, as it would enable a direct comparison of the mechanical performances of different CFBAs.

3.3.2. Effect of coating volume in CFBAs. The volume fraction of the anode coating in CFBAs has been found to be another important factor governing mechanical performance. A modelling study has shown that, for a constant volume of CFBA, increasing the volume ratio of the coating results in an increase in theoretical capacity, but a decrease in the tensile stiffness.[60] This is expected, given that the carbon fibre has a higher axial modulus than the coating, and the coating has a greater

theoretical capacity. Interestingly, however, for a CFBA with a coating volume fraction of 23.4%, the loss in stiffness compared to that of an uncoated carbon fibre was only 12%. This indicates that a relatively high volume loading of coating, and hence an increase in theoretical capacity, can be achieved with only a relatively small reduction in the stiffness of the composite.

The highest coating volume fraction that has been achieved for a CFBA to date is 11%, highlighting that greater volume fractions of the coating need to be targeted in future research, or assembly strategies need to be modified to enable greater volume fractions to be produced. There also needs to be consideration for how CFBAs will interact with the surrounding electrolyte matrix. Modelling has shown that increasing the volume fraction of a CFBA relative to the surrounding matrix increases the reversible capacity, with minimal effect on the stiffness.[60] However, the interfacial mechanical properties between the coated anode material and the matrix are also important and are yet to be explored.

4. Performance of carbon fibre based cathodes

4.1. Introduction to CFBCs

In commercial LIBs, the cathode is the limiting factor due to a lower theoretical capacity of the active material than that of its anode counterpart.[61] This is also the case for carbon fibre based cathodes as the active material used is the same as that in conventional batteries and the carbon fibre is only used as a current collector, with a structural support, as shown in Fig. 2b. Unlike the anode side of the battery, carbon fibres cannot be used for lithium-ion storage as the intercalation potential of the cathode material is higher than that of the fibre. In addition, CFBCs primarily use intercalation-type electrode materials, which have lower theoretical capacities than the conversion-type electrodes seen in CFBAs. Nevertheless, CFBCs provide a significant improvement in terms of mechanical properties for structural cathodes since current state-of-the-art
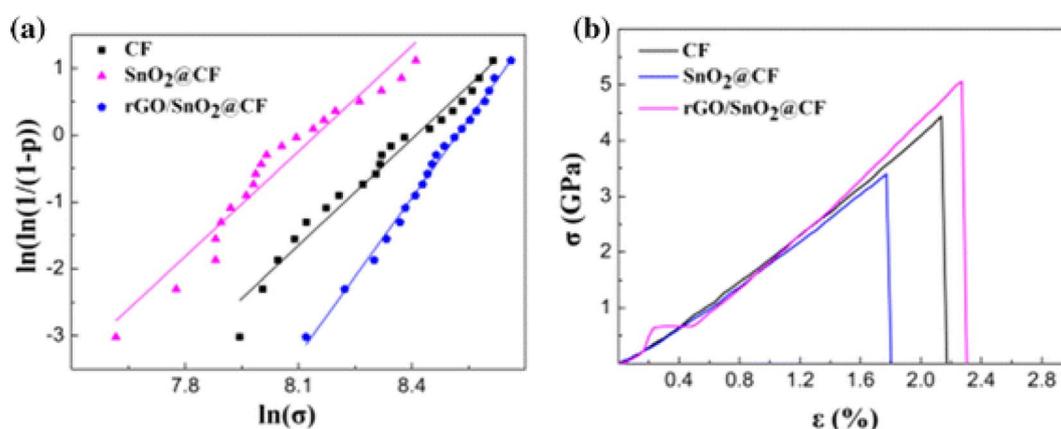

Fig. 7 (a) Weibull plots and (b) stress–strain curves for carbon fibre anodes, a CFBA with a SnO_2 coating, and a CFBA with a SnO_2 and rGO coating.[16] Reproduced from ref. 16 with permission from Springer Nature, copyright 2024.

structural cathodes are simply cathode particles on a metal current collector substrate, as shown in Fig. 2a, which offer little in terms of mechanical properties.[6] This section presents the progress to date on CFBCs, with the scope broadened to include the 2D coating of cathode materials onto carbon fibres.

4.2. Electrochemical properties of CFBCs

4.2.1. Effect of the coating method of CFBCs. The electrochemical properties of CFBCs in the literature are compared in Table 5 which outlines the performance of different assembly strategies and cathode materials. From this comparison, it is clear that two main manufacturing methods are currently used for coating the carbon fibres: EPD and hydrothermal synthesis. There is currently no clear indication of which of these methods, or even a combination leads to superior electrochemical properties. Slurry coating presents an alternative, inexpensive and straightforward approach, but it is only suitable for coating onto flat sheet materials. When used on 3-dimensional (3D) fibres, the surface area available for coating is limited. One of the main outcomes from a comparison of the manufacturing methods is that there is a need for more research into the way in which active cathode materials are coated onto carbon fibres and the effects this has on the storage capability of the cathode.

By comparing the different performances of the cathode coated carbon fibres, it is evident that the performance of the CFRP cathode is primarily determined by the material used, rather than the manufacturing method. There are many other factors that can influence the electrode properties, where the loss of capacity has been widely reported and is affected by a range of variables, such as porosity[72] and thickness[72,73] of the electrode, conductive additive,[73] Li+ ion diffusion[74] and electrolyte properties.[75] Comparing the different coating methods with different electrode materials and charging procedures, such as differing charge rates, the cycling conditions and the materials used result in varied results that cannot be compared. Although the manufacturing method plays a role in the ability for the cathode materials to maintain high performance, the coating method will differ for different materials. The optimal conditions for a specific carbon fibre coating method will vary for each individual cathode material depending on the properties of that cathode. This can lead to certain coating methods being more suitable than others for each cathode. Finding the optimal conditions for each material will require additional research on cathode coating of carbon fibres.

To realise the full potential of a structural battery there is a need to ensure that the cathode coating is optimised for the cathode materials. For example, the slurry coated carbon fibre cathodes are shown to have poor capacity retention, especially at high initial capacities. The slurry coated cathode materials are LFP and nickel-manganese cobalt (NMC), of which the latter is known to degrade easily whilst cycling.[76] Dip-coated fibres,[36] which are only cycled 20 times, and slurry coated fibres[33] both have uneven coating thicknesses across the carbon and only contain carbon black conductive particles. This heterogenous coating thickness, the inclusion of polyvinylidene fluoride (PVDF) as a binder and lack of conductive additives, such as

Table 5 A comparison of the electrochemical performance of several 3D and 2D coated CFBCs

Cathode type	Coating material	Type of carbon fibre	Coating method	Estimated nominal potential vs. Li/Li+	Initial discharge capacity/mA h g⁻¹ (C-rate)	Capacity retention/cycles (C-rate)	Coulombic efficiency (%)	Ref.
LFP	$LiFePO_4$	Unsized single fibres	EPD	3.37 V	131 (0.1C)	91%/500 (1C)	99.90	62
	$LiFePO_4$	Sized single fibres	EPD	3.4 V	110 (0.1C)	62%/500 (1C)	99.80	32
	$LiFePO_4$	Unsized single fibres	Slurry coating (dip-coated)	3.45 V	54.4 (0.2C)	96%/20 (0.2C)	99.4	36
	$LiFePO_4$	Sized woven carbon fibre	Slurry coating	~3.4 V	112 (0.1C)	82%/500 (1C)	~98	33
V_2O_5	V_2O_5	3D carbon matrix support on carbon fibres	Hydrothermal	3.0–4.0 V	360.6 (0.1C)	99.3%/120 (1C)	99.90	63
NMO	$LiNi_{0.5}Mn_{1.5}O_4$	Fibre tow	EPD/hydrothermal	2.8 V & 4.0 V	140 (15 mA g⁻¹/~0.1C)	98%/50 (0.1C)	>90	64
	$LiNi_{0.5(1-x)}Mn_{1.5(1-x/3)}Cr_xO_4$	Carbon fibre paper	EPD/hydrothermal	4.7 V	135 (0.2C)	98%/200 (0.2C)	—	65
LMO	Li_2MnO_3	Single fibres	EPD/hydrothermal	~4.0 V	248.4 (0.04C)	80%/30 (0.1C)	89.90	66
	$LiMn_2O_4$	Carbon fibre paper	Hydrothermal	3.9 V	125 (1C)	93.2%/50 (1C)	92.40	67
	$Li(Mn_{0.97}Al_{0.03})O_2$	Fibre tow	EPD/hydrothermal	3.2 V & 3.9 V	190 (0.5C)	85.1%/150 (0.5)	—	68
	$LiMnO_2$	Carbon cloth	EPD	~3.3 V	254 (1C)	87.6%/1000 (4C)	97	69
NMC	$LiNi_{0.88}Mn_{0.06}Co_{0.06}O_2$	Fibre tow	Slurry coating	3.75 V – 4.17 V	200 (0.2C)	70%/100 (1C)	90.10	70
Conversion	Cu_2S	Carbon fibre paper	Spray pyrolysis	1.73 V – 1.85 V	421 (0.1C)	~80%/100 (1C)	>98	71

graphene oxides, lead to an inability to maintain high capacity retention compared to the electrophoretic deposition samples. These effects can be exacerbated over multiple cycles, as observed by the different LFP capacity retentions in Table 5.

Park et al.[33] used slurry coating to coat LFP particles onto woven carbon fibres with the same precursor material that Hagberg et al.[32] used to coat carbon fibres using EPD. The 2D slurry coated cathode showed improved electrochemical performance compared to the 3D EPD coated sample; however, the coating was more inhomogeneous, as demonstrated in Fig. 8. Ren et al.[70] used a similar method of slurry coating of NMC active particles not just on the surface but throughout a carbon fibre substrate. This NMC cathode material is reported to exhibit poor capacity retention[77] but is shown to have improved cycling performance when combined with carbon fibres; this highlights the importance of having good electrical contact between the active material and carbon fibre.[32]

The inclusion of additives influences the electrochemical performance of the cathode coating. For example, LFP has been coated onto desized fibres by EPD[32,62] with different conductive additives and produced similar nominal potentials. Hagberg et al.[32] used only carbon black as an additive, with PVDF as a binder, and Sachez et al.[62] used a similar EPD procedure and used exfoliated graphene oxide (EGO) as an additional conductive material. It is also worth noting that Sanchez et al.[62] used poly diallyldimethylammonium chloride (PDDA) as a surfactant, a substance that aids in the dispersion of the charged particles, preventing agglomeration. By including the additive in a deposition bath, it eliminated the need for the PVDF binder. For initial discharge levels, the fibre that included

EGO exhibited a superior initial capacity and an improved capacity retention of over 30% compared to the use of a carbon black additive cathode. By using PDDA, a more even and uniform coating was produced and the inclusion of exfoliated graphene oxide improved the electrical connectivity between the LFP particles and carbon fibre current collector, which improved both the coulombic efficiency and overall capacity. The intercalation potential and overpotentials of the two different LFP cathodes are similar, around 3.4 V and ~50 mV respectively,[32,62] indicating that conductive additives and an even coating have little impact on the internal electrical resistance of the electrode. The most discernible difference between the electrodes is the storage capacities, where the EGO containing electrode showed a high capacity approaching 130 mA h g^{-1}, compared to a maximum of 108 mA h g^{-1} for the electrode without EGO. This effect was even more apparent at high C-rates, where the EGO-based sample's capacity was ~70 mA h g^{-1}, over double that of the sample without EGO at ~30 mA h g^{-1}. Despite both systems exhibiting high coulombic efficiencies, with the EGO electrode having an efficiency of 99.9% compared to the carbon black electrode having 99.8% efficiency, the fibre with EGO showed improved long-term capacity retention, as it retained 88% of its capacity compared to the electrode without EGO, which only retained 66% of its original capacity over 500 cycles at 1C. This demonstrates the necessity for a highly connected electrical network within the electrode coating to access the lithium within the cathode particles.

Excessive electrochemical degradation and capacity loss can be attributed to not only the pre-treatment processes, but also to
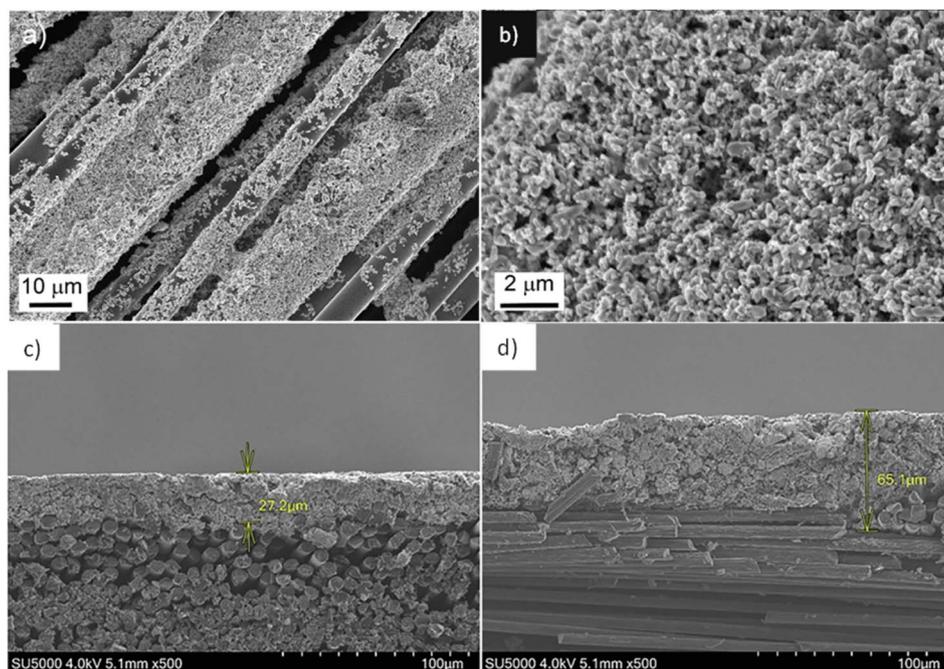

Fig. 8 (a) and (b) Scanning electron microscopy (SEM) images of lithium-iron-phosphate (LFP) coated carbon fibres produced using electrophoretic deposition (EPD)[32] and (c) and (d) LFP coated carbon fibres produced using slurry coating.[33] (a) and (b) Reproduced from ref. 32 with permission from Elsevier, copyright 2024. (c) and (d) Reproduced from ref. 33 with permission from Elsevier, copyright 2024.

the electrical connection between the carbon fibres and the active material. Petrushenko et al.[36] used a dip-coating method using only carbon black to connect all of the constituents electronically and, as a result, achieved an initial capacity of 54 mA h g^{-1} and a low retention of 96% at a slow charge rate of 0.2C. Sanchez et al.,[62] demonstrated improved electrochemical properties by EPD coating of an unsized fibre using EPD with exfoliated graphene oxide in addition to carbon black, obtaining a much higher initial capacity of 131 mA h g^{-1}, despite a slower C-rate of 0.1C, and a better capacity retention of 91% at a faster C-rate of 1C. The inclusion of small and highly conductive particles improved the electrochemical capabilities of this cathode, although the effect the coating method has on these properties is less well understood and needs to be explored further to understand how to minimise long term degradation.

EPD deposition time greatly affects electrochemical performance, as shown in Fig. 9 for a LFP-coated CFBC.[62] Fig. 9a shows that the CFBC with the shortest deposition time of five minutes gave the most intense CV peaks and had the shortest spacing between anodic and cathodic peaks. Fig. 9b and c show that the CFBC with the shortest deposition time also had the greatest capacity, at all C-rates. The CFBC with the shortest

deposition rate also has the greatest capacity retention, as shown in Fig. 9d. The improved performance of the CFBC where the coating time was only five minutes was attributed to the fact that the shorter deposition time created a more uniform coating of LFP and EGO on the carbon fibre surface, preventing particle agglomeration.[62]

4.2.2. Effect of pre-treatment for CFBCs. Waller et al.[67] evaluated a range of fibre pre-treatment processes by: (i) curing fibres at 300 °C, led to the functional groups within the sizing to react with both the fibre and with each other, altering the carbon fibre surface,[78,79] and (ii) soaking fibres in the precursor solution before hydrothermal heating. The pre-treatment stage improved the coating homogeneity due to enhanced hydrophilicity, leading to increased capillary action. Zou et al.[63] utilised a 3D networked carbon matrix to encapsulate the V_2O_5 coating, enhancing both electron conductivity and ionic transportation. This resulted in a cathode material demonstrating remarkable performance, with 100% capacity retention over 5000 cycles. Furthermore, the approach effectively mitigated the formation of the solid-electrolyte interface (SEI), a passivating layer notorious for causing capacity fade in LIBs, contributing to the prolonged stability of the electrode.[80] However, to achieve this scaffold for the active nanoparticles, multiple preliminary
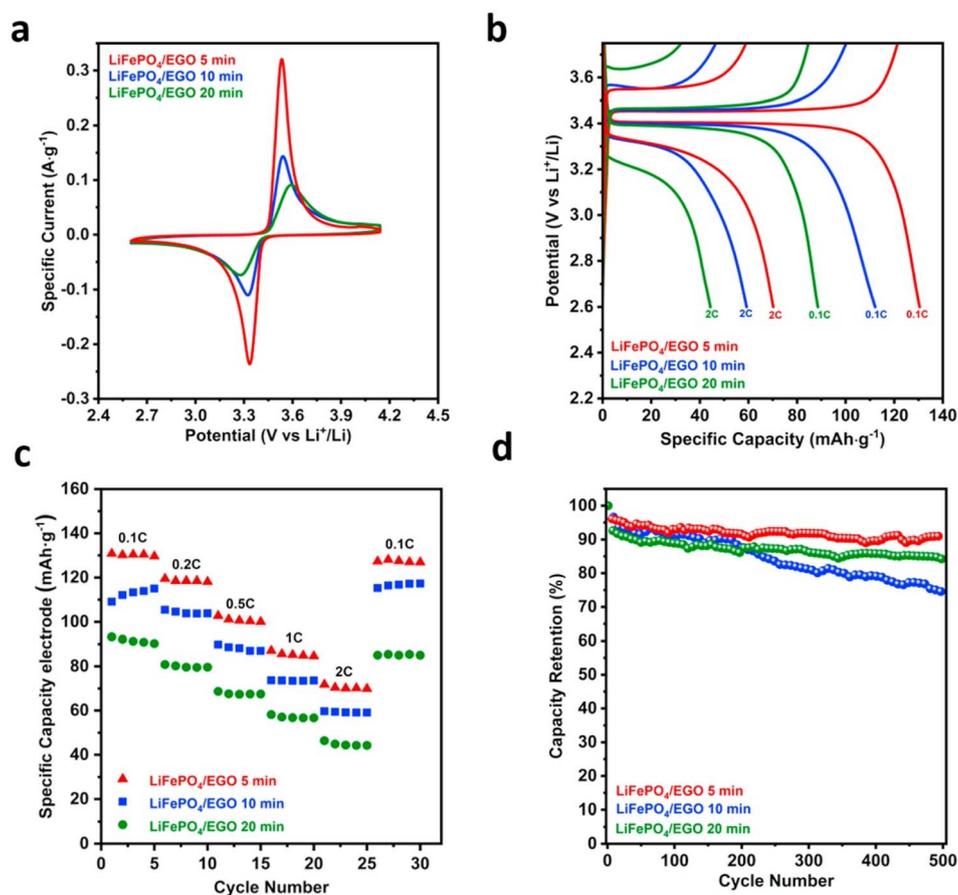

Fig. 9 Plots to compare the electrochemical performance of LFP-coated CFBCs with different deposition times, including: (a) CV, (b) first cycle voltage profile, (c) specific capacities at different C-rates, and (d) capacity retention.[62] Reproduced from ref. 62 with permission from Elsevier, copyright 2024.

steps of sol–gel, acid and heat treatment of the carbon fibre must be performed before the hydrothermal synthesis of the V_2O_5 material is conducted. This represents a time consuming and energy intensive procedure that would be costly to scale up to industrial levels.

Liu et al.[66] demonstrated a combined hydrothermal and electrophoretic deposition coating method, which exhibited a large initial reduction in capacity, (49.1 mA h g^{-1} drop after the second discharge due to a phase transformation) leading to a lower capacity retention than that of the hydrothermally synthesised $LiMn_2O_4$ by Waller et al.[67] Despite this lower capacity retention, the higher initial capacity of the combined method resulted in a higher overall capacity compared to that of the materials produced by the purely hydrothermal method. It is also worth noting that the combined route was evaluated against a graphite anode, rather than against lithium metal, meaning that a capacity loss could occur due to the different anode used in the analysis.

Two examples[64,65] of CFBCs with NMO as the cathode coating exhibited a good capacity retention of ~98% over a minimum of 50 cycles, although at relatively low C-rates. This material is thought to be a more sustainable alternative coating owing to a lack of cobalt and low nickel content with comparable electrochemical properties.[61,81] Doping of the NMO cathode material with a varying amount of Cr was examined by Liu et al.,[65] which demonstrated the flexibility of this coating method to allow selective adaption of the composition of the solution when using hydrothermal synthesis directly on carbon fibres.

4.2.3. Conversion-type cathodes for CFBCs. Most of the cathode materials that have been examined to date belong to the transition metal oxide (TMO) group, $LiMO_x$, (M = Co, Mn, Ni, Fe),[82] which are all intercalation-type cathodes. To improve the reversible capacity of LIBs, conversion-type cathodes such as Cu_2S are also being considered. Cu_2S offers a higher theoretical capacity of 337 mA h g^{-1} and uses less expensive and more abundant elements than intercalation-type TMO cathodes.[82] Kalimuldina et al.[71] coated carbon fibres with Cu_2S, which exhibited an initial discharge capacity of 379 mA h g^{-1} at 0.1C, which decreased to 330 mA h g^{-1} after five cycles (98% of its theoretical capacity) and 311 mA h g^{-1} after 50 cycles; these capacity values are higher than that of most TMO materials. Even at a charging rate of 1C, the performance showed little capacity fade after the first few cycles. However, it is important to note the significantly lower voltage range, between 1.0 and 3.0 V, compared to the higher nominal voltages seen in TMO cathodes, which are above 3.0 V.

The initial discharge capacity of Cu_2S of 415 mA h g^{-1} rapidly decreased to 280 mA h g^{-1} after three cycles; however this capacity could be maintained for a further 97 cycles with 100% coulombic efficiency. It was found that coating this material on a carbon fibre, rather than non-structural current collectors such as aluminium foil, improved capacity loss due to the superior electron pathway and lower resistance of corrosion of the active materials. These results demonstrate the advanced capabilities of carbon fibres as a current collector for different types of new and novel cathode materials.

4.3. Mechanical properties of CFBCs

Studies on the mechanical properties of CFBCs are limited, with the only existing study investigating the adhesion between the coating and the carbon fibre for LFP particles coated on carbon fibres using EPD.[32] Three-point bending testing suggested that the adhesion between the coating and the carbon fibre is sufficiently high to support load transfer through the interface. Double cantilever beam testing indicated that the quality of the interfaces in the CFBC is comparable to the quality of those in a carbon fibre and epoxy composite. It is recommended that the thickness of the coating layer be investigated in future experiments, which was also recommended for CFBAs.

5. Beyond Li-ion technology for CFBEs

Although most research into CFBEs has focused on Li-ion technology, several other chemistries have also been explored. This brings the benefits of bifunctionality provided by structural batteries to other battery types. Chen et al.[83] used hydrothermal synthesis to produce a MnO_2 coated carbon fibre CFBC, that was combined with a Zn metal coated CFBA to form a full Zn–MnO_2 structural battery cell. The MnO_2-based CFBC was produced using a hydrothermal synthesis method on desized carbon fibres, as this technique is known to generate a layered structure that provides a higher capacitance than when using EPD.[84]

In this study Zn–MnO_2 was found to have a reversible capacity of 181.5 W h kg^{-1}, or 145.9 mA h g^{-1}, at a current density of 0.1 A g^{-1}. The reversible capacity was shown to degrade drastically when the current density was doubled to 0.2 A g^{-1}, decreasing by almost a third to 108.0 mA h g^{-1}. The cell showed a promising capacity retention of 88.3% after 100 cycles and 50.2% capacity retention after 500 cycles at 0.1 A g^{-1}. The full battery was also tested for its mechanical properties, with failures resulting from the poor contact between the two working electrodes.

The final electrochemical and mechanical properties of the Zn–MnO_2 structural battery are presented in Table 6, where they are compared to those of a state-of-the-art Li-ion structural battery that consisted of a LFP coated Al foil cathode and a carbon fibre anode separated by a glass fibre separator,[6] as outlined in Fig. 10. Notably neither electrode is a CFBE. The plain weave Li-ion structural battery showed improved Young's modulus compared to a Zn–MnO_2 battery; however, the Zn–MnO_2 battery showed greater electrochemical performance. The specific power of the Zn–MnO_2 battery was more than seven times greater than that of the plain weave Li-ion structural battery, although the Zn–MnO_2 battery was cycled at a slightly lower C-rate. In addition to the difference in C-rates of the two cells, it is worth noting that the testing was undertaken on two cells with different coating thicknesses, different electrolytes, and different full cell assembly architectures, which makes it difficult to properly compare these structural batteries. The next section discusses the challenges associated with the assembly of full cells composed of CFBEs.

Table 6 A comparison of the electrochemical and mechanical properties of a Zn-ion and Li-ion structural battery

	Mechanical properties		Electrochemical properties (full cell)	
	Young's modulus (GPa)	Tensile strength (MPa)	Energy density (W h kg^{-1})	Specific power (W kg^{-1})
Siraj et al.[6] Li-ion GF plain weave 0°/90° separator	25.7	>213	41.2 (0.05C)	12.4 (1C)
Siraj et al.[6] Li-ion Whatman GF/A	11.5	>118	25.9 (0.05C)	8.5 (1C)
Chen et al.[83] Zn–MnO$_2$ (woven)	12.8	293.4	55 (0.69C[a])	93.9 (0.69C[a])

[a] C-rate calculated based on maximum battery capacity.

Sodium-ion batteries tend to have lower gravimetric densities due to their higher mass as well as a higher reduction potential, resulting in less energy per sodium ion. However, carbon fibres have been tested as a support material for sodium batteries. MoS$_2$ anode nanosheets have been successfully grown on the surface of carbon fibres, showing improved electrochemical capabilities and capacity retention, even at elevated C-rates, compared to the MoS$_2$ nanosheets without the carbon fibre.[85] Electrospinning of SnO$_2$ nanoparticles in PAN followed by heat treatment to form composite nanofibers enables embedding of SnO$_2$ particles in these carbon nanofibers for use as an anode material in a Na-ion battery. This, in turn, creates a flexible and free standing electrode without the need for a binder or conductive additives.[86] Similarly, V$_2$O$_5$ nanosheets can be coated onto carbon fibres using hydrothermal synthesis and used as an anode material in Na-ion batteries, with potential application as a CFBA.[53]

By creating a carbon fibre with an alternative structure, it is possible to adapt the functionality of the fibre to improve its ability to uptake ions. For example, electrospun lignin fibres can be used to form carbon fibres that are capable of being cycled with a Na metal counter electrode with a maximum initial capacity of 310 mA h g^{-1}.[87] Changing the carbonization temperature during the manufacturing was shown to affect maximum capacity and cyclability,[88–90] with a lower temperature (800 °C) leading to higher capacity but an increased capacity loss over extended cycling. This is thought to be due to increased levels of Na ions being lost due to more SEI formation at lower carbonization temperatures. However, if the carbonization is too high (1700 °C), this can lead to sodium ions being
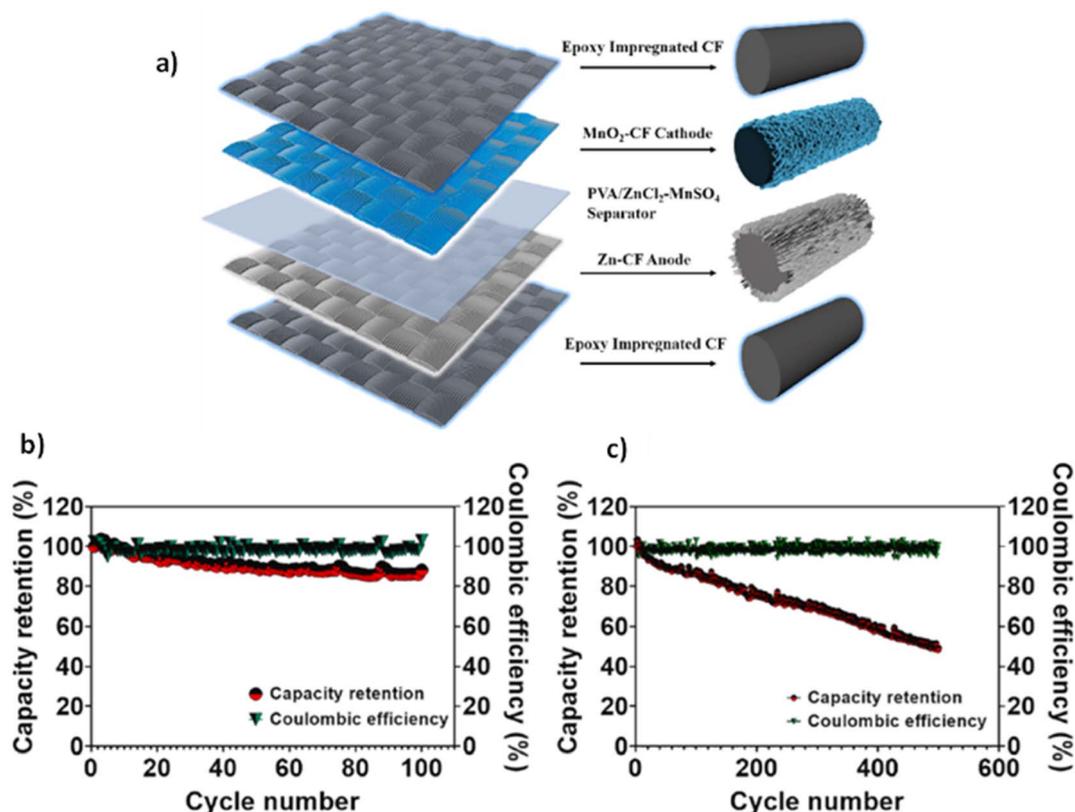

Fig. 10   (a) Schematic of a full structural Zn–MnO$_2$ composite battery. (b) Electrochemical cycling tests of a Zn–MnO$_2$ battery for 100 cycles and (c) 500 cycles.[83] Reproduced from ref. 83 with permission from Elsevier, copyright 2024.

trapped in defects, similar to that observed in hard carbons. Obtaining a balance between the higher and lower carbonization temperatures was found to result in an optimised system.

Although not able to produce the micron length-scale carbon fibres used in previously discussed structural batteries, electrospinning polyacrylonitrile (PAN) creates sub-micron length fibres, which can incorporate specific particles. These fibres can improve performance of particles that are usually prone to large volume changes and therefore mechanical deformation. This was shown by Fu et al.,[91] who observed that iron-sulfide particles (for K-ion batteries, as opposed to Li-ion batteries) suffered from pulverisation and deactivation due to structural changes. However, when the particles were incorporated into the electrospun fibres, Fu et al.[91] found that it was possible to maintain the morphology due to this "fully wrapped" architecture that protects these particles.

Metal-air batteries utilise atmospheric molecules as an external cathode to significantly reduce the weight of the system resulting in a higher energy density. However, the anode materials usually consist of metals, such as sodium and zinc, increasing the weight and cost of the battery. Carbon fibres, with a heterogenous surface that allow the OER/ORR (Oxygen Evolution Reaction/Oxygen Reduction Reaction) to occur, provide a viable alternative with enhanced capabilities. This has been achieved through oxidation of the carbon fibre surface using a combination of H_2O_2 and concentrated H_2SO_4, followed by heating at high temperatures under H_2.[92] Use of carbon fibres allows for a flexible air battery by using a thin zinc counter electrode that would significantly reduce the weight of an overall system compared to using conventional lithium-ion batteries. Utilizing these as a structural component could further improve this system efficiency but has yet to be tested as such.

Lithium-metal anodes and anode-free batteries have become a more widely researched topic in recent years due to their high capacity and voltage potential. In anode-free batteries, carbon fibres can be used as a substrate for plating with Li metal, where the application of a highly conductive and homogenous Li metal coating can immensely improve the capacity and cyclability of the electrode. For example, using a facile co-deposition synthesis route to deposit NiCo nanocubes evenly across the 3D skeletal structure of a carbon fibre composite resulted in a smooth coating with a high surface area that allowed for plating and stripping of lithium metal with high-coulombic efficiency.[93] This self-supported electrode was also found to be flexible and self-healing, able to remove almost all Li at low voltages and perform at different bending angles. A similar procedure for coating high-entropy metal alloys on carbon fibers was developed by Wang et al.[94] that allowed for homogeneous Li nucleation and uniform Li deposition. This allows for a highly reversible lithium plating/stripping process to occur over 2000 cycles with a coulombic efficiency of 99.6% at a low C-rate and 99.5% at 1C over 160 cycles.

Flexible batteries have gathered a lot of attention recently as they meet the needs of wearable electronics, flexible sensors, and complex designs. Carbon nanofibers are a key candidate material for use as an anode in flexible batteries and supercapacitors due to their high porosity, electrical conductivity,

and mechanical properties.[95] Utilising carbon fibres as an anode material provides multiple benefits beyond energy storage, as outlined by Zenkert et al.[96] It allows for strain sensing through the piezo-electrochemical transducer (PECT) effect, whereby a change in the open-circuit potential is observed when mechanical stress is applied to the cell. In the case of a lithiated carbon fibre, the amount of strain is directly related to the magnitude of the voltage change. This effect could also be used for energy harvesting by applying a mechanical load to an already lithiated carbon fibre, increasing the voltage of the cell before being discharged. The energy harvesting is facilitated by the losses in mechanical work from the reversible insertion strain in the carbon fibres by the Li-ions.

6. Considerations for the production of full CFBE cells

6.1. Full cell assembly

Although significant attention has been given to improving the interfacial properties between the carbon fibre and CFBE coatings, in particular in the pre-treatment stage, there are currently no publications on the interface between the coating and the surrounding solid matrix in a structural battery. Matrix materials in state-of-the-art structural batteries are biphasic, consisting of a mechanically strong, porous polymer phase with an ionically conducting liquid solvent percolating through it that allows for Li^+ transport.[97] The electrolyte is created by introducing a monomer-containing liquid to the electrode layup which then undergoes thermally initiated polymerisation to produce the porous polymer phase, in a process called polymerisation-induced phase separation.[98]

It is known that there is good adhesion between the biphasic electrolyte and carbon fibre anodes in current state-of-the-art SBs;[99,100] however, it is difficult to predict the strength of the adhesion between the biphasic electrolyte and the electrode coating. The current practice for CFBE studies is to chop the CFBE into short pieces and combine it with a conductive additive and a binder in a slurry for characterisation in a coin cell.[16] This setup is not representative of a CFBE in a real structural battery which consists of continuous unidirectional or woven carbon fibres surrounded by a biphasic matrix. Future studies should combine the CFBE as continuous carbon fibres with a biphasic electrolyte and undertake electrochemical and mechanical testing, since this will provide a true representation of the performance in a real structural battery cell. In the future, the production of full cells containing CFBEs and the laminated architecture would also aid with earlier detection of other important issues related to full cells including balancing of electrodes, efficient current collection, and accounting for volume changes in different materials.

6.2. Full cell disassembly

Recycling of structural batteries is particularly challenging as individual recycling processes for both commercial LIBs and carbon fibre composites are currently widely recovering all materials.[101] The additional challenge that is specific to the

recycling of CFBE-based structural batteries is the recovery of carbon fibres in a state where the electrode coating has been removed or does not compromise the safety or performance of the carbon fibres in their recycled application.

One strategy is to leverage advances in commercial LIB recycling using electrode coatings that are commonly used in commercial LIBs and are therefore the focus of existing recycling methods, such as LFP and NMC.[102] For example, pyrometallurgical recovery is a common commercial LIB recycling method that uses high temperatures to recover metals such as Co, Fe and Ni as an alloy.[103] Hydrometallurgical recovery can then be used to recover individual metals from the alloy using solvents, such as the use of H_2SO_4 and H_2O_2 to recover Co from an alloy of Ni, Mn and Co.[104] These processes could be adapted to remove the electrode coating from carbon fibres in CFBE-based structural batteries. A disadvantage of this strategy is that the use of NMC is undesirable due to supply risks associated with Co.[105]

Pyrolysis is a recycling method used to recover carbon fibres from carbon fibre composites using high heat treatment temperatures to remove the matrix.[101] A post-gasification step is often required to remove a layer of char from the carbon fibre after pyrolysis. This step has been shown to result in a 20% loss in Young's modulus and tensile strength,[106] limiting the effectiveness of the carbon fibre in future applications. This presents potential challenges when using pyrometallurgical recovery as part of the carbon fibre recycling processes. These factors highlight the importance of using sustainable and non-toxic electrodes in CFBE-based structural batteries. Reuse should also be considered, and is likely challenging for CFBE-based structural batteries as the high adhesion required between components in the composite would make it difficult to replace or regenerate individual components. Full cells could however be reused in second-life applications such as stationary energy storage when they are no longer sufficiently energy dense for transport applications due to capacity fade.

7. Conclusions

This review has provided an overview of carbon fibre based electrodes as next generation materials for future structural batteries. The energy density of structural batteries is currently 41 W h kg^{-1} and needs to be further increased in order to be considered for more challenging applications, such as future electric aircraft. To address this challenge, carbon fibre based electrodes offer a pathway to achieve this with carbon fibre based anodes possessing energy densities of up to 829 mA h g^{-1}, compared to 177 mA h g^{-1} for current carbon fibre anodes, and carbon fibre based cathodes offering a route to create the first truly structural cathode material.

With respect to the anode side of the structural battery, a wide range of high energy density and relatively sustainable anode materials have been explored including: Fe_3O_4, Zn_xO_y and NiO. Good electrochemical performance has been achieved through the high surface area coating of energy dense conversion-type anode materials onto carbon fibres that alleviates detrimental volume changes in the anode material during cycling. On the cathode side of the battery, studies on carbon fibre based cathodes are more limited; however, a number of commercial cathode materials have been coated onto carbon fibres including lithium-iron-phosphate (LFP) and nickel-manganese-cobalt (NMC), with a reversible capacity of 110 mA h g^{-1} achieved for LFP which is respectable compared to the theoretical value of 170 mA h g^{-1}. It is clear that the manufacturing method plays a role, at least indirectly, in the ability of the cathode materials to maintain high capacity retention, even at elevated C-rates. A number of other factors, such as the cathode material itself, the pre-deposition treatments and the additives included must be considered when creating a coating process.

Several knowledge gaps in the literature have been found for carbon fibre based electrodes, most notably the limited number of studies on mechanical properties upon lithiation, which are critical to structural batteries due to their load bearing function. Existing results on mechanical properties are promising, with an Mn_3O_4 coated carbon fibre exhibiting just an 8% and 6% loss in tensile strength and elastic modulus, respectively, compared to a pristine carbon fibre. Further research needs to be undertaken to understand and optimise the balance between electrochemical and mechanical performance for carbon fibre based electrodes.

The assembly and end-of-life processes for carbon fibre based electrodes have also been considered. Electrophoretic deposition is being highlighted as a favourable option for electrode assembly due to its potential for scalability, relatively low cost, and low energy requirements. Another important consideration for the assembly which has not yet been studied is the interface between the electrode and the electrolyte matrix, as this is critical to both the mechanical and electrochemical performance of the composite. The limited potential for recycling of these materials is also noted; however, existing recycling processes in both the Li-ion battery and carbon fibre space may be able to be leveraged in order to recover materials from or find secondary applications for carbon fibre based electrodes. Addressing a number of these challenges can provide a route to create structural batteries for applications, including those for challenging applications such as transport.

For a broader perspective on the future development of structural batteries, a more inclusive focus on architecture that takes into account the need for recyclability needs to be developed. With new opportunities to redesign the makeup of these batteries with new materials, it is important that failures observed in both current commercial Li-ion batteries and carbon fibre composites are addressed. Having a more modular approach that allows for the separation of individual components could provide a route for easier recycling of the materials used within these batteries. Additionally, the use of novel coating techniques that are more sustainable, such as low-solvent and spray coating of fibres with an active material would improve the overall carbon footprint of these batteries, whilst reducing their costs significantly.

Data availability

No primary research results, software or code have been included and no new data were generated or analysed as part of this review.

Conflicts of interest

There are no conflicts of interest to declare.

Acknowledgements

References

1 W. Johannisson, D. Zenkert and G. Lindbergh, *Multifunct. Mater.*, 2019, **2**, 035002.

2 P. Ladpli, R. Nardari, F. Kopsaftopoulos and F. K. Chang, *J. Power Sources*, 2019, **414**, 517–529.

3 L. E. Asp, M. Johansson, G. Lindbergh, J. Xu and D. Zenkert, *Funct. Compos. Struct.*, 2019, **1**, 042001.

4 J. Frazelle, *Commun. ACM*, 2021, **64**, 52–59.

5 G. J. H. Lim, K. K. Chan, N. A. A. Sutrisnoh and M. Srinivasan, *Mater. Today Sustain.*, 2022, **20**, 100252.

6 M. S. Siraj, S. Tasneem, D. Carlstedt, S. Duan, M. Johansen, C. Larsson, J. Xu, F. Liu, F. Edgren and L. E. Asp, *Adv. Energy Sustain. Res.*, 2023, 2300109.

7 L. E. Asp, K. Bouton, D. Carlstedt, S. Duan, R. Harnden, W. Johannisson, M. Johansen, M. K. G. Johansson, G. Lindbergh, F. Liu, K. Peuvot, L. M. Schneider, J. Xu and D. Zenkert, *Adv. Energy Sustain. Res.*, 2021, **2**, 2000093.

8 F. L. Matthews and R. D. Rawlings, *Composite Materials: Engineering and Science*, Woodhead Publishing, Cambridge, 1999.

9 A. E. Scholz, A. Hermanutz and M. Hornung, *Dtsch. Luft- und Raumfahrtkongress 2018*, 2018.

10 F. Liu, D. Wang, J. Liu, H. Wei, H. Zhang, J. Xu, S. Li, Z. Qin, R. Wang, H. Jia and J. Zhang, *J. Phys. Conf.*, 2020, **1637**, 12027.

11 M. Feng, S. Wang, Y. Yu, Q. Feng, J. Yang and B. Zhang, *J. Electrochem. Soc.*, 2016, **163**, A2225–A2231.

12 B. H. Eckstein, *Fibre Sci. Technol.*, 1981, **14**, 139–156.

13 M. Giorcelli, S. Guastella, P. Mandracci, Y. Liang, X. Li and A. Tagliaferro, *AIP Conf. Proc.*, 2018, **1981**, 1–5.

14 M. Feng, S. Wang, Y. Yu, Q. Feng, J. Yang and B. Zhang, *Appl. Surf. Sci.*, 2017, **392**, 27–35.

15 M. Feng, S. Wang, J. Yang and B. Zhang, *J. Mater. Chem. A*, 2016, **4**, 18524–18531.

16 H. Li, S. Wang, M. Feng, J. Yang and B. Zhang, *J. Mater. Sci.*, 2018, **53**, 11607–11619.

17 H. Li, S. Wang, M. Feng, J. Yang and B. Zhang, *Chin. Chem. Lett.*, 2019, **30**, 529–532.

18 Q. Han, X. Zhang, W. Zhang, Y. Li and Y. Sheng, *J. Electroanal. Chem.*, 2020, **871**, 114355.

19 Q. Han, X. Zhang, W. Zhang, Y. Li and Z. Zhang, *J. Alloys Compd.*, 2020, **842**, 155743.

20 Q. Han, F. Wang, Z. Wang, Z. Yi, Z. Na, X. Wang and L. Wang, *Ionics*, 2018, **24**, 1049–1055.

21 Q. Han, W. Zhang, Z. Han, S. Niu, J. Zhang, F. Wang, X. Li, D. Geng and G. Yu, *Ionics*, 2019, **25**, 5333–5340.

22 Q. Han, M. Shi, Z. Han, W. Zhang, Y. Li, X. Zhang and Y. Sheng, *Ionics*, 2020, **26**, 5935–5940.

23 Q. Han, W. Zhang, Z. Han, F. Wang, D. Geng, X. Li, Y. Li and X. Zhang, *J. Mater. Sci.*, 2019, **54**, 11972–11982.

24 Q. Han, Y. Sheng and X. Zhang, *New J. Chem.*, 2021, **45**, 15808–15817.

25 Q. Han, Z. Yi, F. Wang, Y. Wu and L. Wang, *J. Alloys Compd.*, 2017, **709**, 227–233.

26 Q. Han, X. Li, F. Wang, Z. Han, D. Geng, W. Zhang, Y. Li, Y. Deng, J. Zhang, S. Niu and L. Wang, *J. Electroanal. Chem.*, 2019, **833**, 39–46.

27 S. Yao, G. Zhang, X. Zhang and Z. Shi, *Ionics*, 2020, **26**, 5923–5934.

28 F. Stojcevski, T. B. Hilditch, T. R. Gengenbach and L. C. Henderson, *Composites, Part A*, 2018, **114**, 212–224.

29 Q. Wu, M. Li, Y. Gu, S. Wang, L. Yao and Z. Zhang, *Polym. Compos.*, 2016, **37**, 254–261.

30 M. H. Kjell, E. Jacques, D. Zenkert, M. Behm and G. Lindbergh, *J. Electrochem. Soc.*, 2011, **158**, A1455.

31 E. A. M. Hassan, L. Yang, T. H. H. Elagib, D. Ge, X. Lv, J. Zhou, M. Yu and S. Zhu, *Compos. B Eng.*, 2019, **171**, 70–77.

32 J. Hagberg, H. A. Maples, K. S. P. Alvim, J. Xu, W. Johannisson, A. Bismarck, D. Zenkert and G. Lindbergh, *Compos. Sci. Technol.*, 2018, **162**, 235–243.

33 H. W. Park, M. S. Jang, J. S. Choi, J. Pyo and C. G. Kim, *Compos. Struct.*, 2021, **256**, 112999.

34 P. Benedek, N. Wenzler, M. Yarema and V. C. Wood, *RSC Adv.*, 2017, **7**, 17763–17767.

35 M. Faraji Niri, C. Reynolds, L. A. Román Ramírez, E. Kendrick and J. Marco, *Energy Storage Mater.*, 2022, **51**, 223–238.

36 D. Petrushenko, Z. Rahmati, D. Barazanchy, W. De Backer, W. E. Mustain, R. E. White, P. Ziehl and P. T. Coman, *Energy Fuel.*, 2023, **37**, 711–723.

37 J. Hagberg, S. Leijonmarck and G. Lindbergh, *J. Electrochem. Soc.*, 2016, **163**, A1790.

38 G. Fredi, S. Jeschke, A. Boulaoued, J. Wallenstein, M. Rashidi, F. Liu, R. Harnden, D. Zenkert, J. Hagberg, G. Lindbergh, P. Johansson, L. Stievano and L. E. Asp, *Multifunct. Mater.*, 2018, **1**, 015003.

39 Y. Wang, Z. X. Huang, Y. Shi, J. I. Wong, M. Ding and H. Y. Yang, *Sci. Rep.*, 2015, **5**, 1–8.

40 P. Subalakshmi and A. Sivashanmugam, *ChemistrySelect*, 2018, **3**, 5040–5049.

41 F. Wang, Q. Han, Z. Yi, D. Geng, X. Li, Z. Wang and L. Wang, *J. Electroanal. Chem.*, 2017, **807**, 196–202.

42 V. K. H. Bui, T. N. Pham, J. Hur and Y. C. Lee, *Nanomaterials*, 2021, **11**(8), 2001.

43 H. Liu and J. Wang, *Electrochim. Acta*, 2013, **92**, 371–375.

44 M. Zheng, H. Tang, L. Li, Q. Hu, L. Zhang, H. Xue and H. Pang, *Adv. Sci.*, 2018, **5**, 1700592.

45 D. Zhan, X. Yuan, C. Xiang, J. Lu, G. Dai, R. Hu, Z. Xiao, H. Mao, M. Fehse, A. J. Simpson and B. Wu, *Sustain.*

Mater. Technol., 2021, **29**, DOI: 10.1016/j.susmat.2021.e00322.

46 K. Kim, G. Daniel, V. G. Kessler, G. A. Seisenbaeva and V. G. Pol, *Nanomaterials*, 2018, **8**, 1–12.

47 Y. Song, J. Hwang, S. Lee, B. Thirumalraj, J. H. Kim, P. Jenei, J. Gubicza and H. Choe, *Adv. Eng. Mater.*, 2020, **22**, 1–8.

48 Y. Lu, L. Yu and X. W. David Lou, *Chem*, 2018, **4**, 972–996.

49 Y. Ma, Y. Ma, G. Giuli, T. Diemant, R. J. Behm, D. Geiger, U. Kaiser, U. Ulissi, S. Passerini and D. Bresser, *Sustain. Energy Fuels*, 2018, **2**, 2601–2608.

50 M. Singh, J. Kaiser and H. Hahn, *J. Electrochem. Soc.*, 2015, **162**, A1196–A1201.

51 J. Su, Z. Gao, Y. Xie, Z. Zhang and H. Wang, *Compos. B Eng.*, 2021, **212**, 108733.

52 M. Li, M. Feng, D. Luo and Z. Chen, *Cell Rep. Phys. Sci.*, 2020, **1**, 100212.

53 X. Zhang, X. Liu, C. Yang, N. Li, T. Ji, K. Yan, B. Zhu, J. Yin, J. Zhao and Y. Li, *Surf. Coat. Technol.*, 2019, **358**, 661–666.

54 Z. Deng, H. Jiang, Y. Hu, Y. Liu, L. Zhang, H. Liu and C. Li, *Adv. Mater.*, 2017, **29**, 1603020.

55 J. Chen, Y. Wang, X. He, S. Xu, M. Fang, X. Zhao and Y. Shang, *Electrochim. Acta*, 2014, **142**, 152–156.

56 L. Oar-Arteta, T. Wezendonk, X. Sun, F. Kapteijn and J. Gascon, *Mater. Chem. Front.*, 2017, **1**, 1709–1745.

57 Z. Hu, Y. Fu, Z. Hong, Y. Huang, W. Guo, R. Yang, J. Xu, L. Zhou and S. Yin, *Compos. Sci. Technol.*, 2021, **201**, 1–7.

58 E. Jacques, M. H. Kjell, D. Zenkert and G. Lindbergh, *Carbon*, 2014, **68**, 725–733.

59 S. Duan, A. H. S. Iyer, D. Carlstedt, F. Rittweger, A. Sharits, C. Maddox, K. R. Riemschneider, D. Mollenhauer, M. Colliander, F. Liu and L. E. Asp, *Carbon*, 2021, **185**, 234–241.

60 S. Yin, Z. Hong, Z. Hu, B. Liu, X. Gao, Y. Li and J. Xu, *J. Power Sources*, 2020, **476**, 228532.

61 N. Nitta, F. Wu, J. T. Lee and G. Yushin, *Mater. Today*, 2015, **18**, 252–264.

62 J. S. Sanchez, J. Xu, Z. Xia, J. Sun, L. E. Asp and V. Palermo, *Compos. Sci. Technol.*, 2021, **208**, 108768.

63 R. Zou, Q. Liu, G. He, F. Yuen, K. Xu, J. Hu, I. P. Parkin, C.-S. Lee, W. Zhang, R. Zou, Q. Liu, K. Xu, J. Hu, R. J. Zou, M. F. Yuen, C.-S. Lee, W. Zhang, G. He and P. Parkin, *Adv. Energy Mater.*, 2017, **7**, 1601363.

64 Y. H. Liu, H. H. Lin and Y. J. Tai, *J. Alloys Compd.*, 2018, **735**, 580–587.

65 Y. H. Liu and T. Y. Tsai, *J. Power Sources*, 2021, **484**, 229262.

66 Y. H. Liu, T. Takasaki, K. Nishimura, M. Yanagida and T. Sakai, *J. Power Sources*, 2015, **290**, 153–158.

67 G. H. Waller, S. Y. Lai, B. H. Rainwater and M. Liu, *J. Power Sources*, 2014, **251**, 411–416.

68 J. Yao, K. Nishimura, T. Mukai, T. Takasaki, K. Tsutsumi, K.-F. Aguey-Zinsou and T. Sakai, *ECS Electrochem. Lett.*, 2012, **1**, 83–86.

69 X. Zhu, F. Meng, Q. Zhang, L. Xue, H. Zhu, S. Lan, Q. Liu, J. Zhao, Y. Zhuang, Q. Guo, B. Liu, L. Gu, X. Lu, Y. Ren and H. Xia, *Nat. Sustain.*, 2020, **45**(4), 392–401.

70 D. Ren, Y. Yang, L. Shen, R. Zeng and H. D. Abruña, *J. Power Sources*, 2020, **447**, 227344.

71 G. Kalimuldina and I. Taniguchi, *Electrochim. Acta*, 2017, **224**, 329–336.

72 W. Bauer, D. Nötzel, V. Wenzel and H. Nirschl, *J. Power Sources*, 2015, **288**, 359–367.

73 H. Zheng, J. Li, X. Song, G. Liu and V. S. Battaglia, *Electrochim. Acta*, 2012, **71**, 258–265.

74 C. Heubner, M. Schneider, A. Michaelis, C. Heubner, A. Michaelis, M. Schneider and A. Michaelis Fraunhofer, *Adv. Energy Mater.*, 2020, **10**, 1902523.

75 Y. Yamada and A. Yamada, *J. Electrochem. Soc.*, 2015, **162**, A2406–A2423.

76 T. Li, X. Z. Yuan, L. Zhang, D. Song, K. Shi and C. Bock, *Electrochem. Energy Rev.*, 2019, **31**(3), 43–80.

77 R. Jung, M. Metzger, F. Maglia, C. Stinner and H. A. Gasteiger, *J. Electrochem. Soc.*, 2017, **164**, A1361–A1377.

78 Q. Wu, M. Li, Y. Gu, S. Wang, X. Wang and Z. Zhang, *J. Appl. Polym. Sci.*, 2015, **132**, 41917.

79 P. Kiss, J. Glinz, W. Stadlbauer, C. Burgstaller and V. M. Archodoulaki, *Compos. B Eng.*, 2021, **215**, 108844.

80 M. B. Pinson and M. Z. Bazant, *J. Electrochem. Soc.*, 2013, **160**, A243–A250.

81 G. Liang, V. K. Peterson, K. W. See, Z. Guo and W. K. Pang, *J. Mater. Chem. A*, 2020, **8**, 15373–15398.

82 P. He, H. Yu, D. Li and H. Zhou, *J. Mater. Chem.*, 2012, **22**, 3680–3695.

83 J. Chen, Y. Zhou, M. S. Islam, X. Cheng, S. A. Brown, Z. Han, A. N. Rider and C. H. Wang, *Compos. Sci. Technol.*, 2021, **209**, 108787.

84 X. bo Li and G. ri Xu, *Ceram. Int.*, 2017, **43**, 8963–8969.

85 X. Li, Y. Yang, J. Liu, L. Ouyang, J. Liu, R. Hu, L. Yang and M. Zhu, *Appl. Surf. Sci.*, 2017, **413**, 169–174.

86 M. Dingtao, Y. Ongliang Li, H. Mi, S. Luo, P. Zhang, Z. Lin, J. Li and H. Zhang, *Angew. Chem.*, 2018, **130**, 9039–9043.

87 K. Peuvot, O. Hosseinaei, P. Tomani, D. Zenkert and G. Lindbergh, *J. Electrochem. Soc.*, 2019, **166**, A1984–A1990.

88 R. Harnden, D. Zenkert and G. Lindbergh, *Carbon*, 2021, **171**, 671–680.

89 K. V. Kravchyk and M. V. Kovalenko, *Adv. Energy Mater.*, 2019, **9**(35), 1901749.

90 S. Ghosh, U. Bhattacharjee, S. Patchaiyappan, J. Nanda, N. J. Dudney and S. K. Martha, *Adv. Energy Mater.*, 2021, **11**, 1–11.

91 T. Fu, P.-C. Li, H.-C. He, S.-S. Ding, Y. Cai and M. Zhang, *Rare Met.*, 2023, **42**, 111–121.

92 H. F. Wang, C. Tang, B. Wang, B. Q. Li, X. Cui and Q. Zhang, *Energy Storage Mater.*, 2018, **15**, 124–130.

93 Y.-H. Song, Y.-F. Li, J. Lin, G.-D. Yang, X.-L. Wu, J.-P. Zhang, H.-Z. Sun and L. Zhao, *Chem. Eng. J.*, 2024, **481**, 148478.

94 J. Wang, Y. Wang, X. Lu, J. Qian, C. Yang, I. Manke, H. Song, J. Liao, S. Wang and R. Chen, *Adv. Mater.*, 2024, **36**, 2308257.

95 H. Zhang, X. Zhu, Y. Tai, J. Zhou, H. Li, Z. Li, R. Wang, J. Zhang, Y. Zhang, W. Ge, F. Zhang, L. Sun, G. Zhang and H. Lan, *Int. J. Extrem. Manuf.*, 2023, **5**, 32005.

96 D. Zenkert, R. Harnden, L. E. Asp, G. Lindbergh and M. Johansson, *Compos. B Eng.*, 2024, **273**, 111240.

97 N. Ihrner, W. Johannisson, F. Sieland, D. Zenkert and M. Johansson, *J. Mater. Chem. A*, 2017, **5**, 25652–25659.

98 L. M. Schneider, N. Ihrner, D. Zenkert and M. Johansson, *ACS Appl. Energy Mater.*, 2019, **2**, 4362–4369.

99 J. Xu, W. Johannisson, M. Johansen, F. Liu, D. Zenkert, G. Lindbergh and L. E. Asp, *Compos. Sci. Technol.*, 2020, **188**, 107962.

100 W. Johannisson, N. Ihrner, D. Zenkert, M. Johansson, D. Carlstedt, L. E. Asp and F. Sieland, *Compos. Sci. Technol.*, 2018, **168**, 81–87.

101 E. Pakdel, S. Kashi, R. Varley and X. Wang, *Resour. Conserv. Recycl.*, 2021, **166**, 105340.

102 L. F. Zhou, D. Yang, T. Du, H. Gong and W. Bin Luo, *Front. Chem.*, 2020, **8**, 1–7.

103 G. Harper, R. Sommerville, E. Kendrick, L. Driscoll, P. Slater, R. Stolkin, A. Walton, P. Christensen, O. Heidrich, S. Lambert, A. Abbott, K. Ryder, L. Gaines and P. Anderson, *Nature*, 2019, **575**, 75–86.

104 L. P. He, S. Y. Sun, X. F. Song and J. G. Yu, *Waste Manag.*, 2017, **64**, 171–181.

105 A. Zeng, W. Chen, K. D. Rasmussen, X. Zhu, M. Lundhaug, D. B. Müller, J. Tan, J. K. Keiding, L. Liu, T. Dai, A. Wang and G. Liu, *Nat. Commun.*, 2022, **13**(1341), DOI: **10.1038/s41467-022-29022-z**.

106 J. Yang, J. Liu, W. Liu, J. Wang and T. Tang, *J. Anal. Appl. Pyrolysis*, 2015, **112**, 253–261.